Delft University of Technology

SC42095 CONTROL ENGINEERING

Supersonic Jet (07-20)

Delft, January 7, 2021

Zhehan Li 5217350

Contents

List of Figures

List of Tables

INTRODUCTION

In supersonic jet, pitch angle is defined as the angle between the horizon and the aircraft longitudinal axis. To change the flight level of the flight, either increase altitude (pitch-up) or decrease altitude (pitch-down), the pilot moves the control column, which in turn gives input signals to the actuators to move the elevators. Elevators are the surfaces that move which in turn moves the aeroplane's nose up, or down.

A Supersonic Jet Control System is provided which is modeled as a fourth order transfer function between the pitch angle of the aircraft and the actuator as shown in Equation 0.1.

$$G(s) = \frac{10(s+1)}{s(s+10)(s^2+1.5s+6.25)} \tag{0.1}$$

The fourth order transfer function is used for design and evaluation of the controller in continuous time and discrete time.

In this report, the design of controllers for the given system in continuous time and discrete time are addressed. Classical Control Methods (P, PD, PID etc) and the Modern Control Theory techniques (State Feedback, Output Feedback and LQ control) are used to design the controllers. Simulations are performed using **Matlab** and **Simulink**. This report consists of first 13 sections where each section addresses the corresponding question in the assignment, and last section containing the final conclusion of this report.

1 Continuous Time Controller for Set-point tracking

In this section, the given system is analyzed and a controller is developed for set-point step input tracking utilizing the techniques of Classical Control Engineering. The control objectives for a set-point step are

- Maximum Overshoot of 5%
- Minimal Settling Time
- Zero Steady State Error

The following block diagram denotes schematically the relation between input r and output y,

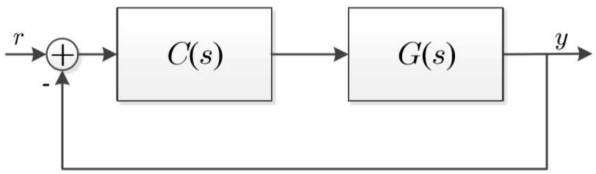

Figure 1.1: Reference set-point step block diagram

here G(s) and C(s) represent respectively the plant and controller transfer functions in Figure 1.1

1.1 System Anatomy

In order to design an effective controller, the fourth order transfer function describing the system is analyzed. The transfer function is reproduced below

$$G(s) = \frac{10(s+1)}{s(s+10)(s^2+1.5s+6.25)} \tag{1.1}$$

The poles and zeros of the transfer function are :

- Poles: 0, -10, -0.7500 ± 2.3848i
- Zeros: -1

Since all the poles and zeros are included in the Left Half Plane (LHP), the system is marginally stable and minimum-phase. The stability of the system can also be affirmed by the positive gain margin (20dB at 3.76 rad/s) and phase margin (96.1 deg at 0.163 rad/s) of the open loop bode diagram of the plant in Figure 1.2.

By applying the final value theorem for steady state error with step input to the reference and C(s) = 1, the steady state error of the system is given by Equation 1.2

$$G(\infty) = \lim_{t\to\infty} e(t) = \lim_{s\to 0} sE(s) = \frac{sR(s)}{1 + \lim\limits_{s\to 0} G(s)} \tag{1.2}$$

- R(s) is the Laplace transform for step input which is $\frac{1}{s}$
- $\lim\limits_{s\to 0} G(s)$ is the DC gain of the forward path transfer function, which is plant system itself.

For the steady state error to be zero, we need the DC gain of forward path transfer function to be infinity. Due to presence of one integrator in the plant transfer function we have the forward path DC gain to be infinity and hence the steady state error is 0, which also corresponds to the type of the plant being N=1 (number of pure integrators).
In this subsection, the stability of the plant system is confirmed. In the next subsections, the controller design for the set-point tracking for the step input is discussed.

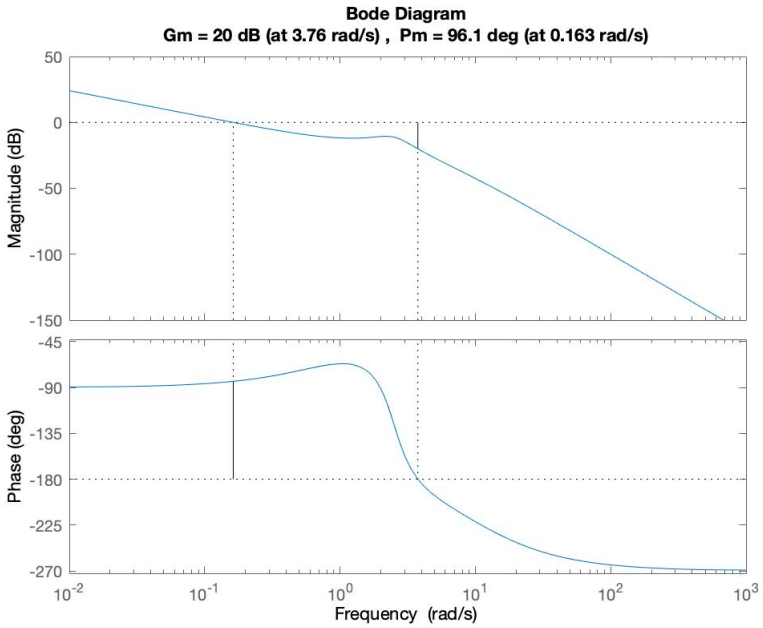

Figure 1.2: Bode Plot of the Plant

1.2 Analysis of Performance Requirements

In this section, the results of different controllers obtained are discussed. **Root Locus** technique has been employed to design a controller which makes the closed loop system stable and meets the control objectives. In order to examine the requirements of the controller gains in frequency-domain, we have to translate the objectives for the performance characteristics of the system in time domain into requirements in the bode plot of the plant. Since the controller is designed in frequency domain, it is natural to first look at the bode plot of the given system. Figure 1.2 shows that the bode plot for the plant has an increase in phase from -90° towards phase peak of -66° due to the zero present at 1 rad/s before it drops down due to damping ratio at 2.5 rad/s and stays at -270°.

- Maximum Overshoot of 5%
  In order to meet the first design requirement, we should find a relationship between the overshoot in time domain and frequency domain peaks. From the book by Horowitz [2], we can relate the overshoot in time domain step response with the damping ratio for a second order system according to:

$$Y(s) = \frac{\omega_n^2}{s^2 + 2\zeta\omega_n s + \omega_n^2} R(s) \tag{1.3}$$

  where ζ is the damping ratio and ω_n the natural frequency, which determines the speed of convergence. The following equations which can be used in combination with the design objectives.

$$overshoot = 100 \cdot e^{\frac{-\zeta\pi}{\sqrt{1-\zeta^2}}} \rightarrow \zeta = \sqrt{\frac{(ln\frac{overshoot}{100})^2}{\pi^2 + (ln\frac{overshoot}{100})^2}} \tag{1.4}$$

  Besides, the phase margin (measured in degrees) of a second-order system can be related with the damping ratio ζ of an under-damped system ($\zeta < 1$) with the following relationship

$$phase\ margin = tan^{-1} \frac{2}{\sqrt{\sqrt{4 + \frac{1}{\zeta^4}} - 2}} \approx 100\zeta \tag{1.5}$$

  where the linear approximation in the RHS of Equation 1.5 is reasonably accurate for $\zeta < 0.7$, which is a useful index for correlating the frequency response with the transient performance of a

system. The linear approximation can also be applied to higher order system as long as we assume that the transient response of the system is primarily due to a pair of dominant under-damped poles [1]. Since in our case, we indeed have a complex pair of dominant poles in the closed-loop transfer function, we can approximate our 4th order system by a dominant second-order system to fairly find an approximation about the desired phase margin in the bode plot and damping ratio. Based on Equation 1.4, the approximate desired damping ratio ζ is computed as

$$\zeta_{des} \approx \sqrt{\frac{(ln\frac{5}{100})^2}{\pi^2 + (ln\frac{5}{100})^2}} \approx 0.6901 \tag{1.6}$$

Then by using Equation 1.5 the approximate desired phase margin is

$$phasemargin_{des} \approx 100 * \zeta_{des} \approx 69\ degrees \tag{1.7}$$

for 2nd order system

With these approximations, we can have a general idea about the desired phase margin of the Loop transfer function L(s) in the coming controller designing procedure, in order to find the appropriate gains of the controller to meet the design criteria.

- Minimal Settling Time
  Wc & WB
  The second requirement for minimal-settling time is strongly dependent on the bandwidth ω_B of the system [3]. Meanwhile, the bandwidth is also correlated with the crossover frequency (ω_c) of the system that larger value of ω_c results in large value of ω_B which is normally quite smaller than ω_c. In general, a large bandwidth corresponds to a faster rise time because high frequency signals are more easily passed on to the outputs. Therefore, in order to obtain the minimal settling time, we should achieve as larger bandwidth as we can to make the system response faster, but not extremely high in order to reject high frequency noise signals.

- Zero Steady State Error
  As illustrated in Equation 1.2, the steady state error is 0 due to presence of one integrator in the plant transfer function, which implies that the integral term I of the PID controller is not needed, despite the fact that an integral term affects also in the overshoot and settling time of a system, as the system has zero steady error without adding any term in the controller and there is no need to increase the order of the system further. We can use a PD controller to speed up the system and decrease the overshoot.

1.3 Controller Design

Since the step response of the plant has no steady state error, the first step in the design of the controller is to introduce a Proportional Controller with a gain Kp. Figure 1.3 shows step responses of the closed loop systems with three different P Controllers respectively. The corresponding statistical information of the step responses are collected in Table 1.1. From the observation of Figure 1.3 and Table 1.1, the requirements of maximum overshoot of 5% and no steady state error can be satisfied by only applying the P Controller with Kp=4.

Table 1.1: Step information of the System with three different P controllers

	Kp=1 (plant)	Kp=4	Kp=6
Rise Time (seconds)	14.6428	0.8796	0.5428
Settling Time (seconds)	26.448	8.9505	14.5774
Overshoot (percentage)	0	0.2749	16.5949
Steady State Value	1	1	1

In order to obtain the minimal settling time, the PD Controller is used to accelerate the system further. The following sub-sections discuss the different controllers used and their results. Matlab's **ControlSystemDesign** was used for root locus which allows to change the controller parameters and view the resulting frequency plot instantaneously easing the iterative procedure involved.

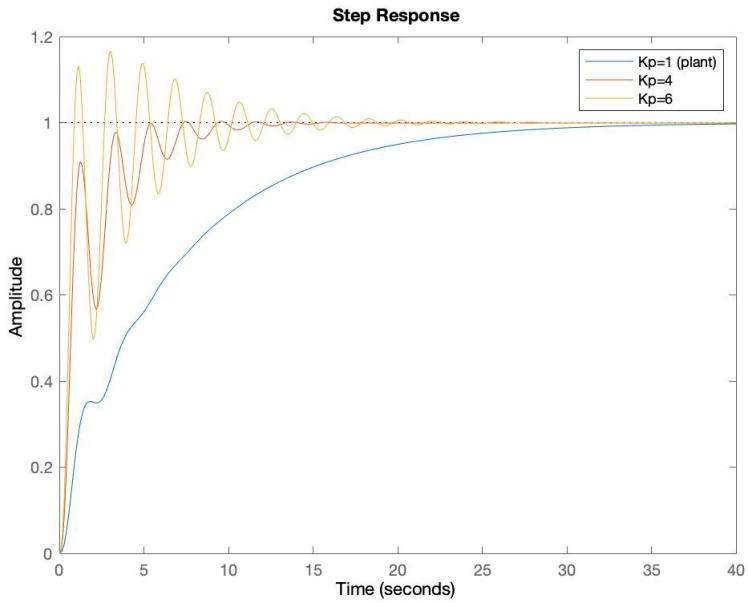

Figure 1.3: Step response of the System with three P controllers

1.4 PD Controller

The ideal PD regulator given by the transfer function $C_{PD}(s) = K_P(1 + sT_D)$ can not be realized, because the pure derivative can not be implemented as it will give a very large amplification of measurement noise in high frequencies. Therefore the approximate realizable phase-lead form, as give in Equation 1.3 is applied in this subsection,

$$\hat{C}_{PD} = A_p \frac{1 + sT_D}{1 + sT} \tag{1.3}$$

with the choice T_D=T_2, where T_2 is the second largest time constant of the process, and the overexcitation $\eta = \frac{T_D}{T}$ [1]. The $\hat{C}_{PD}$ regulator lengthens the higher frequency part of the straight line of slope -20$dB/decade$ by shifting the breakpoint frequency $\frac{1}{T_2}$ to the right to point $\frac{1}{T}$. This improves the phase conditions, to reach a given phase margin the value of crossover frequency (open-loop system bode amplitude crosses 0 dB) can be increased, which results in a faster settling process, which also means that the bandwidth of the system (closed-loop system bode amplitude crosses -3 dB) is increased. The higher the value of the parameter η, the bigger the acceleration. By using the Matlab command **DisplayFormat='time constant'**, we can represent out plant as given in Equation 1.4,

$$G(s) = \frac{0.16(1 + s)}{s(1 + 0.1s)(1 + 0.6(0.4s) + (0.4s)^2)} \tag{1.4}$$

where the first and the second largest time constant in the denominator are T_1=0.4 and T_2=0.1 respectively.

- Initially, in order to examine the characteristics of the PD controller and to determine the desired crossover frequency of the D term, we set $\eta = \frac{T_D}{T} = \frac{T_2}{T}$=5, A_p=1, which can be considered as a typical value but as we don not have any information for the noise of the system or for the limits of actuators, is not possible to confirm if it is acceptable. The resulting controller transfer function is given below in Equation 1.5, followed by the bode plot of open-loop transfer function and step response of the close-loop system in Figure 1.4.

$$G(s) = \frac{(1 + 0.1s)}{1 + 0.02s} \tag{1.5}$$

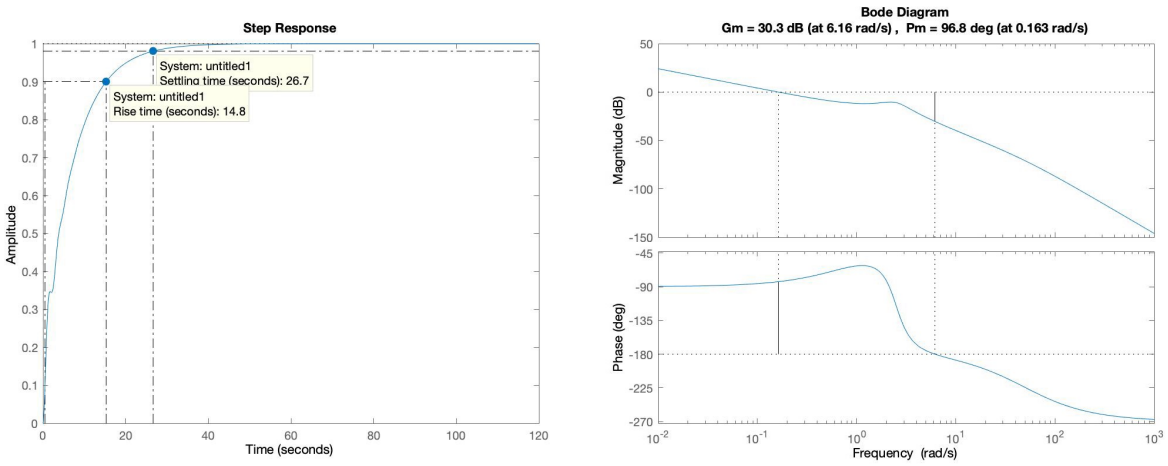

Figure 1.4: Bode plot of loop transfer function (right) and step response of the close-loop system (left) with PD controller in Equation (1.5)

The bode plot given in Figure 1.4 shows that the crossover frequency is in this case does not change at all, and the phase margin and gain margin are still positive. The step response given in Figure 1.4 shows that the settling time is 26.7s with zero overshoot. This implies that we can accelerate the system further by increasing η and A_p to obtain a larger ω_c.

- With $T_d = T_2 = 0.1$, $\eta = \frac{T_D}{T} = 10$, $A_p = 5$, the new controller transfer function is given below in Equation 1.6, followed by the bode plot of loop transfer function and step response of the close-loop system in Figure 1.5.

$$C(s) = 5\frac{(1+0.1s)}{1+0.01s} \tag{1.6}$$

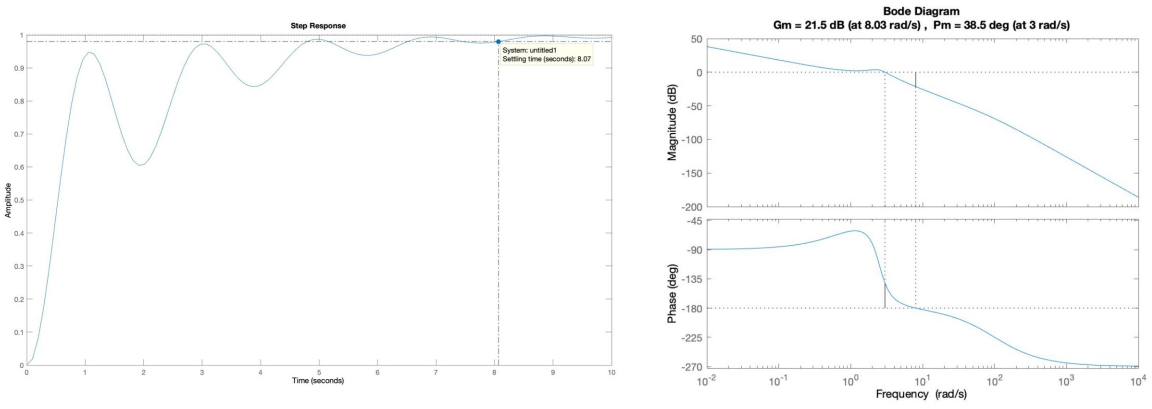

Figure 1.5: Bode plot of loop transfer function (right) and step response of the close-loop system (left) with PD controller in Equation (1.6)

From the bode plot in Figure 1.5, it can be verifed that by increasing A_p and η, the crossover frequency is increased to 3 rad/s with positive phase margin and gain margin. The step response given in Figure 1.5 shows that the settling time is 8.07 s with zero overshoot.

1.5 Modification to the PD Controller

In the previous section, two realizable PD Controllers were designed which met the control objectives

(overshoot less than 5%, no steady state error). In this subsection, an iteration procedure has been implemented with the aim of satisfying all the design criteria of the controller. For each iteration was constructed a step response plot and a bode plot, and all the performance characteristics in time and frequency domain of the system were recorded. All the results of this procedure are represented in the Table 1.2.

Table 1.2: Iterations to tune A_p, T_d and η of PD Controller

Iteration	A_p	T_d	η	P.O(%)	S.T(s)	PM(deg)	ω_c(rad/s)	GM	ω_d(rad/s)
1	10	0.1	10	25.5	8.9	17.2	3.85	15.4	5.42
2	6.07	0.1	10	3.6	7.71	30.4	3.22	19.8	0.27
3	5	0.2	10	0	7.56	46.2	3.13	28.7	0.662
4	10	0.2	10	17.5	4.88	28.2	4.11	22.7	6
5	6.85	0.4	7	4.68	6.21	39.7	4.1	16.5	1.05
6	9	0.5	10	4.77	6.37	49.4	5.26	31.9	8.01
7	8.6	0.6	10	4.59	5.79	50.5	5.63	29.5	8.7
8	8.7	0.5	50	4.19	5.58	49.8	5.16	26.5	8.2
9	9.3	0.5	100	**4.65**	**5.38**	50.3	5.36	51.3	8.12

From the results, one can notice that all the steps were done carefully by taking into consideration all the effect of each term of the controller to the performance characteristics.

- For the first two iterations, the value of A_p was tuned based on the improvement of the performance characteristics in time-domain. We adapted the size of the steps of the increasing to guarantee the stability of the system and faster response. Too large gain value, in the first iteration, resulted in large overshoot and worse settling time compared to previous results.

- To increase the crossover frequency, T_d was increased with corresponding proper gain value A_p during the 3th-7th iteration. By increasing T_d from 0.1 to 0.6, the settling time was decreased dramatically from 7.71 s to 4.59 s with overshoot less than 5%. The acceleration of the system can also be illustrated from the increased ω_c from 3.22 rad/s to 5.63 rad/s and ω_d from 5.42 rad/s to 8.12 rad/s.

- Since the control effort is not limited in this section, we accelerated our system further by increasing η from 10 to 100 during the last two iterations [1]. Finally after the realization of this iteration procedure, a relatively good solution about the parameters of the controller is found by the 9th iteration. The settling time with at least 1% tolerance is 5.38 seconds, which is a very quick response to track the step signal and is clearly satisfactory for the supersonic pitch angle control system. The values of the phase margin and gain margin are both positive and larger than 50, which implies the system has a relatively strong stability property.

By conclusion, the designed PD controller in Equation 1.7 meets all the performance criteria for steady state error, overshoot and settling time and of course is extremely effective in reference tracking which is the main goal of the whole design. The step response and bode plot of the open loop transfer function is shown in Figure 1.6, and the bode plot of the closed loop system is shown in Figure 1.7, from which bandwidth can be observed.

$$G(s) = 9.3\frac{(1+0.5s)}{1+0.005s} = 9.3(1+\frac{0.495s}{0.005s+1}) \tag{1.7}$$

[1] The over excitation value η here is well above the upper limit in most practical applications, and readers are suggested to test this value when designing controllers.

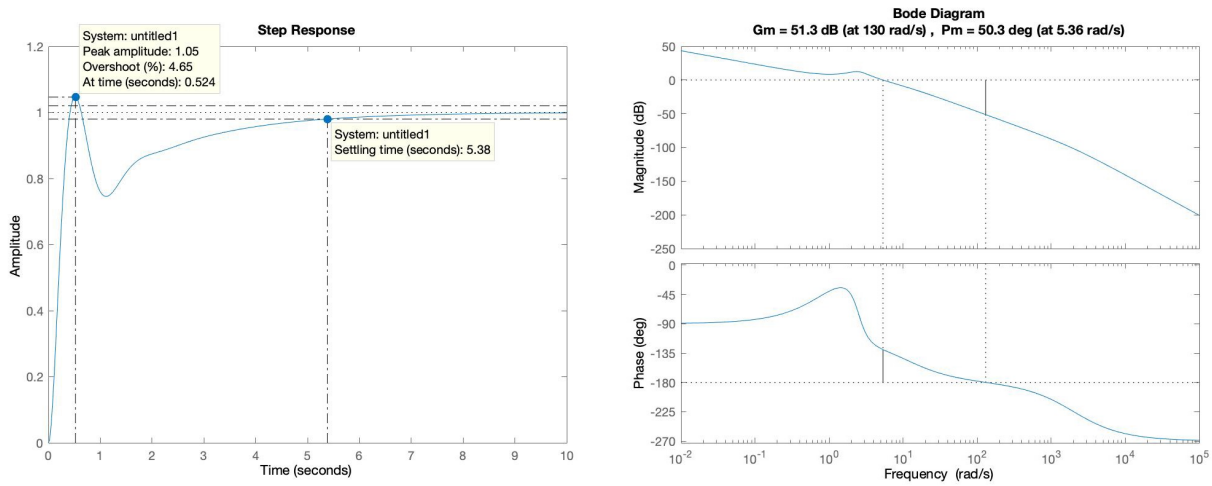

Figure 1.6: Bode plot of loop transfer function (right) and step response of the close-loop system (left) with PD controller in Equation (1.7)

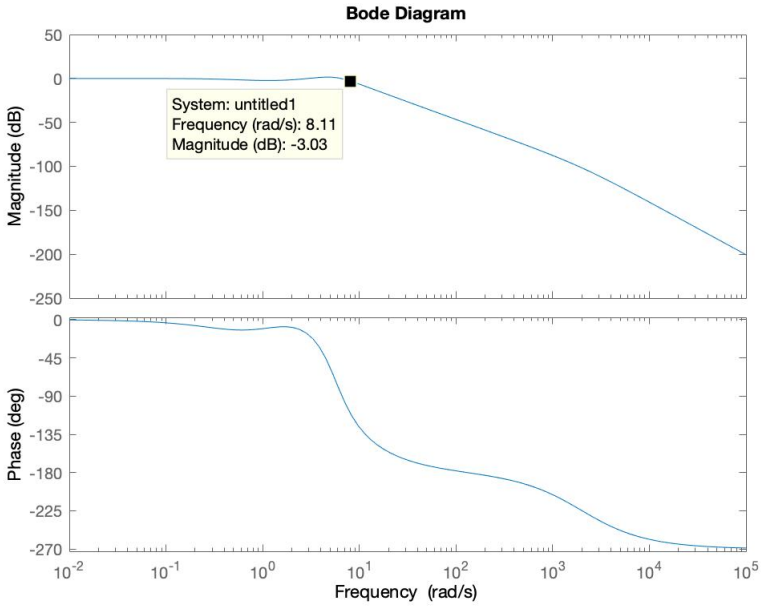

Figure 1.7: Bode plot of the closed-loop system with PD controller in Equation (1.7)

.

2 Disturbance Rejection using Continuous Time Controller

In this subsection instead of the reference set-point change, a step is added to the input of the system as a load disturbance q. The following block diagram describes the system.

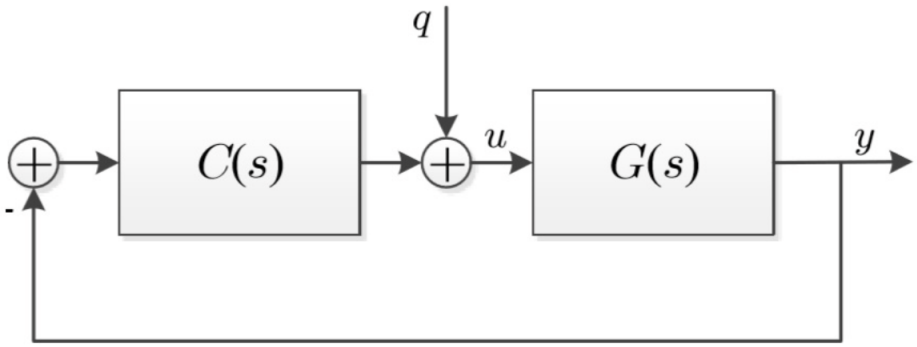

Figure 2.1: Disturbance rejection block diagram

The control objective is to reduce and eliminate the effect of this disturbance as well as possible. This means:

- Minimal amplitude of the system output y caused by disturbance q
- Minimal duration of the disturbance
- No offset caused by the disturbance

2.1 Translation of control objective

From the block diagram in Figure 2.1 the closed loop transfer function is derived:

$$Y(s) = \frac{G(s)}{1 + G(s)C(s)}Q(s) = \frac{G(s)}{s(1 + G(s)C(s))} \tag{2.1}$$

It is required that the the output y(t) equal zero at steady state. Using the final value theorem we obtain:

$$\lim_{t\to\infty} y(t) = \lim_{s\to 0} sY(s) = \lim_{s\to 0} \frac{G(s)}{1 + G(s)C(s)} = \lim_{s\to 0} \frac{\frac{10(s+1)}{s(s+10)(s^2+1.5s+6.25)}}{1 + \frac{10(s+1)}{s(s+10)(s^2+1.5s+6.25)}C(s)} = \lim_{s\to 0} \frac{0.16}{s + 0.16C(S)} \tag{2.2}$$

from which appears clearly that the controller must have an integrator to be able to reject the disturbance step signal and leads the output to zero steady-state offset. Therefore, the first step was to apply a PI controller with standard form in Equation 2.3,

$$C_{pi}(s) = A_p(1 + \frac{1}{sT_I}) = K_I\frac{1 + sT_I}{s} \tag{2.3}$$

2.2 Controller design

With the choice A_p=1, T_I=max$\{T_i\}$=0.4, the largest time constant of the process can be cancelled. In general, PI regulator ensures a high gain in the low frequency domain. The integrating effect increases the type number of the control system by 1. By appropriately placing the cut-off frequency, a stable control system can be obtained with the required phase margin. As the cut-off frequency can not be put into the high frequency domain, the control system will be slow [1]. Figure 2.2 shows the bode plot of the PI Controller (in blue) and Open-loop System (in red), where the w_c is 0.749 rad/s.
In order to increase the w_c so that the phase can be added before the w_c and the response of the

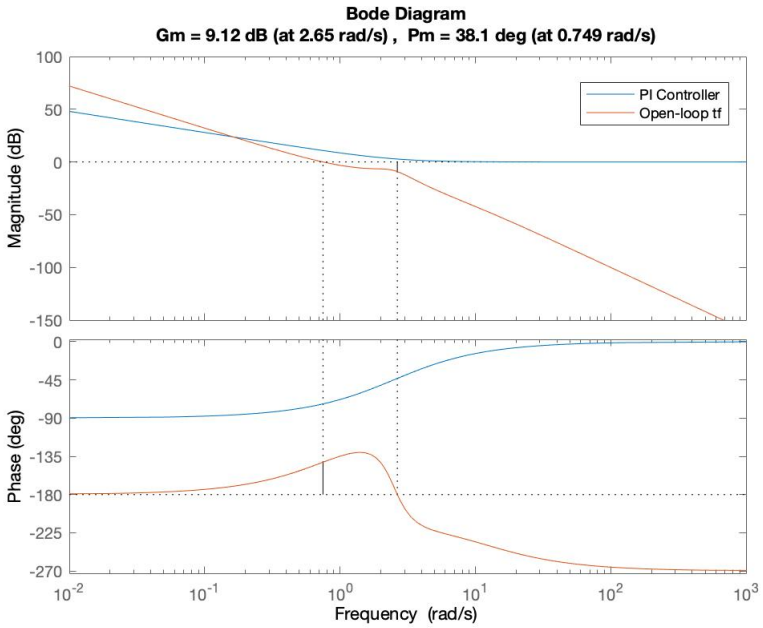

Figure 2.2: Bode plot of Loop transfer function with PI controller for: $A_p = 1, T_I = 0.4$

system can be accelerated further, we decided to apply a PID controller with a first-order derivative filter to reject the disturbance effectively. The standard form of a realizable PID controller with a first-order derivative filter is described as follows:

$$C_{pid}(s) = K_p(1 + \frac{T_d s}{\frac{T_d}{N}s + 1} + \frac{1}{T_i s}) \tag{2.4}$$

with T_i=max{Ti}=T_1 and T_d=T_2. By this structure, the regulator has two poles, one at the origin and another one at $\frac{-1}{T}$, and the straight line section of slope -20 dB/decade on the bode diagram of the loop transfer function is lengthened by the maximal possible extent provided as shown in Figure 2.3 [1]. The maximum phase that PID controller can add is 90 degree for large N in frequencies between the second zero and pole $\frac{1}{T}$ of the transfer function of the controller. The control objectives in this section can be translated into the requirements of bode plot of the loop transfer function in frequency domain that the bode plot is expected to have large gain in low frequencies, large crossover frequency to have a quick rejection of input (small settling time) and $|L(s)|$ should roll faster at higher frequencies.

2.3 PID tuning Iteration

In order to choose the right parameter values based on the interaction of these parameters to the shape of the controller phase, an iterative tuning procedure should be implied as in section 1, which connects the loop transfer function and the performance characteristics in time and frequency domain. For each iteration, the disturbance rejection response and corresponding bode plot were constructed, and all the performance characteristics in time and frequency domain of the system were recorded. All the results of this procedure are represented in the Table 2.1,

- During the first iteration, T_i=T_1=0.4, T_d=T_2=0.1, K_p=1 and N=10 are decided to exam the space of improvement for each parameters. The system rejects the disturbance very slow with M.D.D.=14.1 seconds and a large amplitude of M.A.=0.29, which is definitely not required for the supersonic system. By checking the bode plot, we can find that the peak of the controller phase is far away from the crossover frequency ω_c which is 0.738 rad/s, so the PID controller can not add phase to the system before the ω_c, which implies that the cut-off frequency of the derivative term should

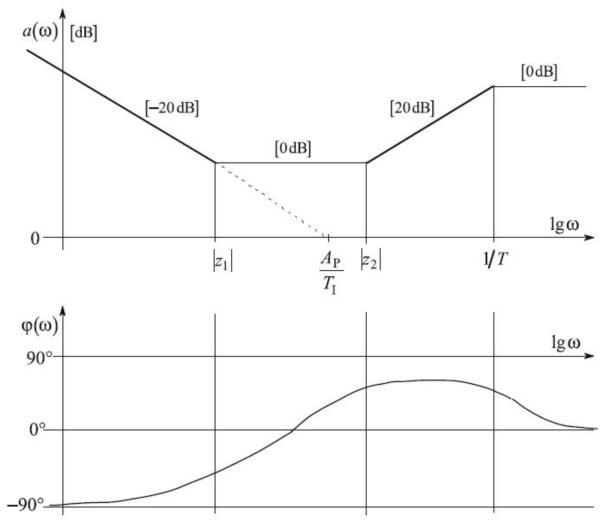

Figure 2.3: Asymptotic Bode diagram of the approximate PID regulator [1]

Table 2.1: Iterations to tune K_p, T_i, T_d and N of PID Controller

Iteration	K_p	T_i	T_d	N	M.A.	M.D.D.(s)	PM(deg)	ω_c(rad/s)	GM
1	1	0.4	0.1	10	0.29	14.1	38	0.738	12
2	10	0.4	0.1	10	NAN	NAN	-16.2	3.82	-7.98
3	1	0.4	0.2	10	0.284	17.6549	38	0.728	42.3
4	20	0.4	0.2	10	0.0493	9.8725	8.59	5.21	16.2
5	40	0.4	0.2	10	0.026	3.8365	11	7.72	10.2
6	40	0.4	0.35	10	0.0192	2.6446	11.1	10.4	4.62
7	40	0.4	0.35	20	0.018	2.6510	20.7	10.3	10.4
8	40	0.4	0.35	35	**0.0178**	**2.6326**	25.1	10.3	15.1

Where M.A. is the maximum amplitude of the response and M.D.D is the minimal duration of the disturbance with 1% tolerance.

become much smaller i.e the T_d term should be increased. Furthermore the proportional gain can be increased with the aim of increasing the crossover frequency. Therefore, in the next iterations, we can increase the ω_c by increasing K_p and T_d.

- By increasing K_p from 1 to 40 and T_d from 0.1 to 0.35 during the 2th-6th iterations, the crossover frequency ω_c increases effectively from 0.738 rad/s to 10.4 rad/s. Consequently, the system response is accelerated (with M.D.D=2.6446 s) and stabilized (M.A.= 0.0192). However, the phase margin and gain margin are not large enough to ensure the robustness and stability of the system for potential disturbances with larger amplitude. During the 7th-8th iterations, the value of N is increased in order to improve the phase margin and gain margin.

- Finally after 8 iterations, a relatively good solution about the parameters of the controller has been found. It is clear from the results, that all the steps were done carefully by taking into consideration all the effect of each term of the controller to the performance characteristics. The duration of the disturbance with at least 1% tolerance of the maximal value of the amplitude, is about 2.6326 seconds, which guarantees that the Supersonic control system has the ability to rejects the disturbance step input relatively very quickly. In addition, the maximum amplitude of the system output y caused by disturbance step input is just only 0.0178, which implies that the disturbance almost does not affect the operation of the system. The performance characteristics in the frequency domain are also satisfying as the GM is equal to 15.1 and PM equal to 25.1 deg. Remarkable is the fact that with this design of controller a large crossover frequency has been achieved as is 10.3 rad/s and is the reason of course for the fast rejection of the disturbance. As it is expected the steady state offset of the output is zero due to the action of the integral term.

Overall, all the design objectives has been satisfied successfully and the PID regulator is able to eliminate the effect of the disturbance which is acting to the pitch angular system of supersonic jet, almost to minimum.

2.4 Design summary

The final transfer function of the PID controller is expressed in Equation 2.5, and the step response for disturbance rejection of closed-loop system with the final design of PID controller is shown in Figure 2.4. The bode plot of Loop transfer function L(s) with the final design of PID controller is provided as well in Figure 2.5.

$$C_{pid}(s) = 40(1 + \frac{0.35s}{\frac{0.35}{35}s + 1} + \frac{1}{0.4s}) = \frac{100(1 + 1.08(0.3795s) + (0.3795s)^2)}{s(1 + 0.01s)} \tag{2.5}$$

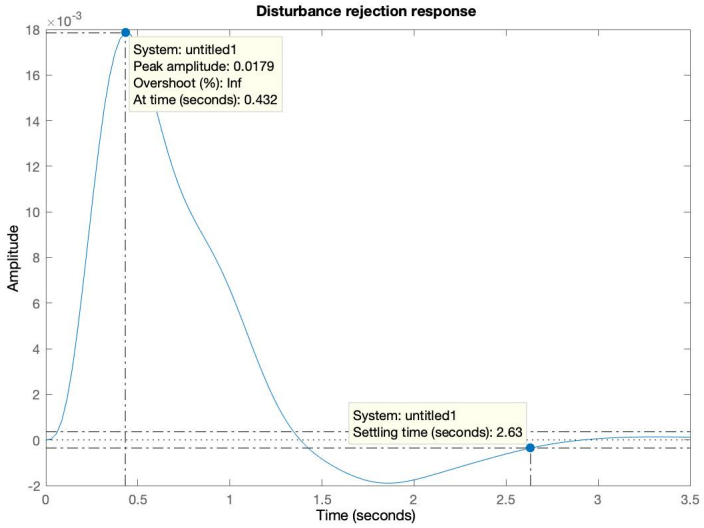

Figure 2.4: Step response for disturbance rejection of closed-loop system with the final design of PID controller

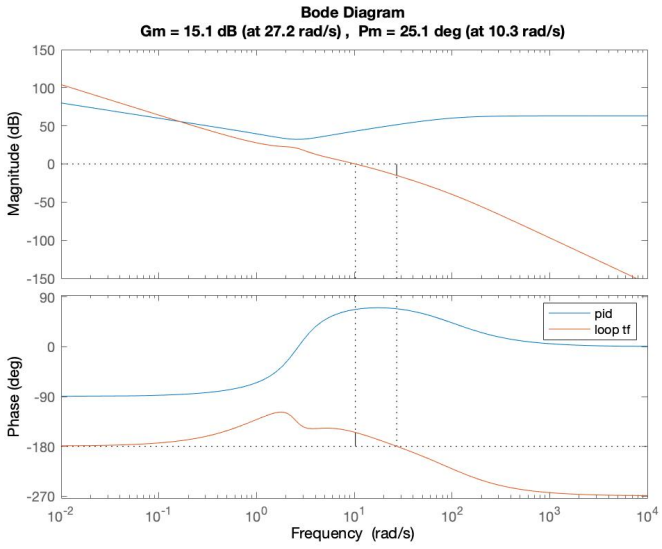

Figure 2.5: Bode plot of Loop transfer function L(s) with the final design of PID controller

3 State Space Notation in Continuous and Discrete Time

The realization of the SISO transfer function to a state-space model can easily be done with a controllable canonical realization and has the following form

$$H(s) = \frac{n_1 s^3 + n_2 s^2 + n_3 s + n_4}{s^4 + d_1 s^3 + d_2 s^2 + d_3 s + d_4} \tag{3.1}$$

$$\dot{x}(t) = \begin{bmatrix} -d_1 & -d_2 & -d_3 & -d_4 \\ 1 & 0 & 0 & 0 \\ 0 & 1 & 0 & 0 \\ 0 & 0 & 1 & 0 \end{bmatrix} x(t) + \begin{bmatrix} 1 \\ 0 \\ 0 \\ 0 \end{bmatrix} u(t) \tag{3.2}$$

$$y(t) = [n_1 \;\; n_2 \;\; n_3 \;\; n_4] x(t) \tag{3.3}$$

For our current system, after filling in the parameters we get the state space model in controllable canonical form. We also use the Matlab command **ss**, whose result agrees with the following matrices.

$$A = \begin{bmatrix} -11.5 & -21.5 & -62.5 & 0 \\ 1 & 0 & 0 & 0 \\ 0 & 1 & 0 & 0 \\ 0 & 0 & 1 & 0 \end{bmatrix} \quad B = \begin{bmatrix} 1 \\ 0 \\ 0 \\ 0 \end{bmatrix} \quad C = [0 \;\; 0 \;\; 10 \;\; 10] \;\; D = 0 \tag{3.4}$$

The physical meaning of the states can be interpreted as follows

$$x = \begin{bmatrix} x_1 \\ x_2 \\ x_3 \\ x_4 \end{bmatrix} = \begin{bmatrix} pitch\ angular\ jerk\ of\ the\ aircraft \\ pitch\ angular\ acceleration\ of\ the\ aircraft \\ pitch\ angular\ velocity\ of\ the\ aircraft \\ pitch\ angular\ position\ of\ the\ aircraft \end{bmatrix} \tag{3.5}$$

When discretizing the system only the A and B matrices need to change and the C and D matrices can be copied this gives rise to the following discrete state space system

$$x_{k+1} = \Phi x_k + \Gamma u_k \tag{3.6}$$

$$y_k = C x_k + D u_k \tag{3.7}$$

where $\Phi = e^{Ah}$, $\Gamma = \int_0^h e^{As} ds B$, with h as the sampling time [3]. Selecting an appropriate sampling period h is done via the Heuristics from lecture 3 slide 11, they are the following

$$N_r = \frac{t_r}{h} \approx 4 - 10 \tag{3.8}$$

where t_r is the rise time to a step input. The rise time found in section 1 was $t_r = 0.2746$ s, and the following $N_r = 8$ was selected which gave satisfying result. This becomes more evident in the next question when step responses are compared. The sampling time of

$$h = \frac{t_r}{N_r} = \frac{0.2746}{8} = 0.034325s \tag{3.9}$$

and the following discrete system was found by the Matlab function **c2d** with zero order hold (ZOH)

$$\Phi = \begin{bmatrix} 0.6639 & -0.6324 & -1.765 & 0 \\ 0.02824 & 0.9886 & -0.03235 & 0 \\ 0.0005176 & 0.03419 & 0.9996 & 0 \\ 6.117 * 10^{-06} & 0.0005879 & 0.03432 & 1 \end{bmatrix} \quad \Gamma = \begin{bmatrix} 0.02824 \\ 0.0005176 \\ 6.117 * 10^{-06} \\ 5.351 * 10^{-08} \end{bmatrix} \quad C = [0 \;\; 0 \;\; 10 \;\; 10] \;\; D = 0 \tag{3.10}$$

The reader is advised to compute their own discretized matrices because the numerical accuracy is very important to get a similar result.

4 Discretization of Continuous time controllers

The continuous time controllers developed for set-point tracking and disturbance rejection in section 1 and 2 respectively are discretized in this section using a sampling interval of h = 0.034325 s. The Matlab command **c2d** was used for discretization of the plant and the controllers with the **Tustin** bi-linear approximation. This method relates the s-domain and z-domain transfer functions using the approximation:

$$z = \frac{1 + \frac{sh}{2}}{1 - \frac{sh}{2}} \tag{4.1}$$

This method of conversion was here preferred because it does not introduce a phase lag [4]. If the zero order hold approximation was used to convert the plant and controllers transfer function, as done with the state space representation in section 3, the output of the system will deteriorate and the controllers should be designed again.
The discrete time transfer function of the plant is given in Equation 4.2, transfer function of the controller for set-point step tracking is given in Equation 4.3 and the transfer function of the controller for disturbance rejection is given in Equation 4.4. All the transfer functions are obtained from their continuous counterparts using the sampling period of h = 0.034325 seconds. The reader is advised to compute their own discretized transfer functions.

$$G(z) = \frac{6.17 * 10^{-5} z^3 + 0.0001663 z^2 - 0.0001668 z - 4.979 * 10^{-5}}{z^4 - 3.652 z^3 + 4.98 z^2 - 3.002 z + 0.6739} \tag{4.2}$$

$$C_{sp}(z) = \frac{272.3 z - 254.2}{z + 0.9434} \tag{4.3}$$

$$C_{dr}(z) = \frac{557.1 z^2 - 1058 z + 505.3}{z^2 - 0.7363 z - 0.2637} \tag{4.4}$$

In Figure 4.1 (left) the reference set-point step responses of the discrete time and continuous time system are compared. The controller assures again a fast convergence without significant overshoot and zero steady state error. In Figure 4.1 (right) the disturbance rejection is shown. For both cases, the discretized responses are following perfectly the continuous time responses without any deviation from the trajectory of the output. Undoubtedly the choice of the sampling time was successful as the discrete time responses for both cases are capturing the dynamics of the response precisely.

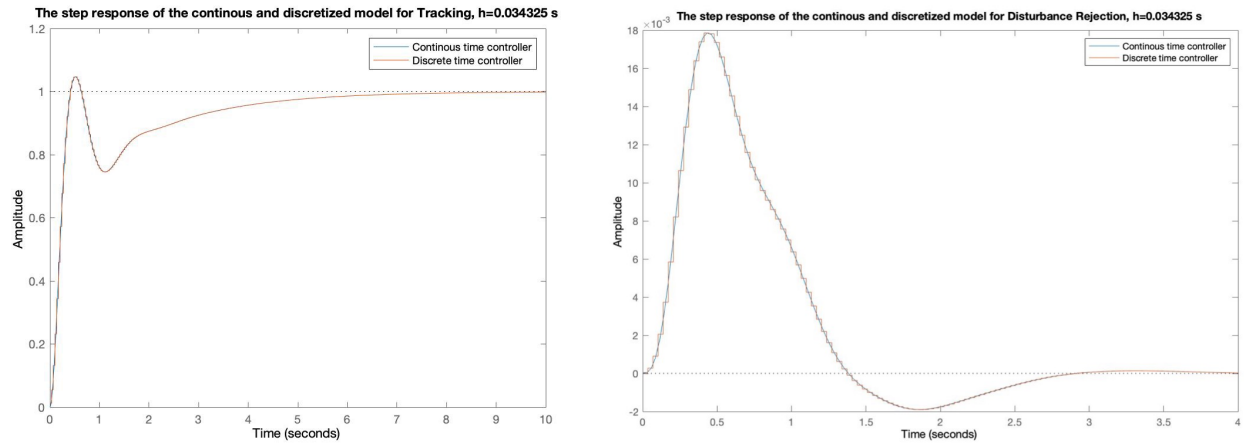

Figure 4.1: Reference set-point step(left) and Disturbance rejection(right) in discrete time and continuous time.

5 Pole Placement Servo Tracking

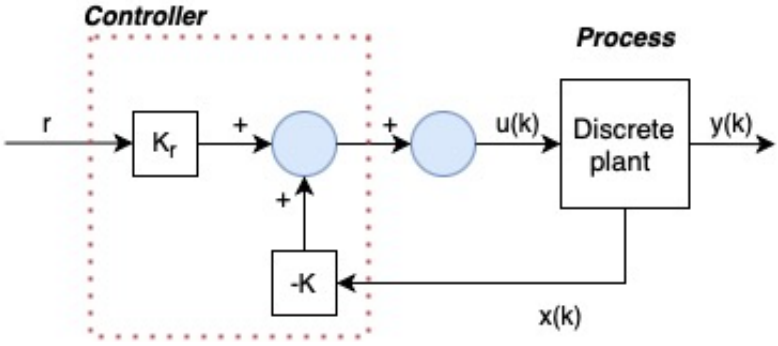

Figure 5.1: Pole placement block diagram

In this section, state feedback controller is developed using pole placement technique for the discrete plant given by Equation 4.2. Figure 5.1 is a diagram of a typical control system using state feedback. The full system consists of the process dynamics, the controller elements K and kr , and the reference input (or command signal) r. The goal of the feedback controller is to regulate the output of the system y such that it tracks the reference input. The control law is here restricted to be linear, and it can be written as

$$u(k) = -Kx(k) + kr * r \tag{5.1}$$

The term $kr * r$ represents a feedforward signal from the reference to the controller. We attempt to determine the feedback gain K so that the closed loop system has a desired characteristic polynomial, which can simply be obtained through Ackermann's formula [3]. Note that kr does not affect the stability of the system but does affect the steady-state solution. In particular, the equilibrium point and steady-state output for the closed loop system are given by

$$x_e = (\Phi - \Gamma K)^{-1}\Gamma kr * r \quad y_e = Cx_e \tag{5.2}$$

hence kr should be chosen such that y_e = r. Being a scalar we can easily solve and show that

$$kr = \frac{-1}{C(\Phi - \Gamma K)^{-1}\Gamma} \tag{5.3}$$

is exactly the inverse of the zero frequency gain of the closed loop system.

The sampling period used here is h=0.0768 seconds. The Matlab command **ctrb** was used to get the Controllablity Matrix or the Kalman matrix which was found to be of full rank. Hence the pair (Φ, Γ) is controllable. In the following, different controllers are obtained by placing the desired poles of the closed loop system at different regions within the unit disc in z-plane. Matlab command **place** was used to compute the feedback gain. In each of these controllers, the closed loop transfer function $G_{cl}(z)$ was obtained and its DC gain was calculated using the Matlab command **dcgain**. The inverse of the DC gain of the closed loop pulse transfer function was then used as the feed forward term for set-point tracking controller.

5.1 Fast system response

In this section, all poles are real and are the faster modes so that the system exhibits a relatively fast response. The poles location is p_f=[0.2, 0.25, 0.3, 0.35]. The step response of the closed loop system is shown in Figure 5.2, where it shows a very high overshoot (peak amplitude of 135 and overshoot of 13400% from the steady state value) and a settling time of 0.0186 seconds.

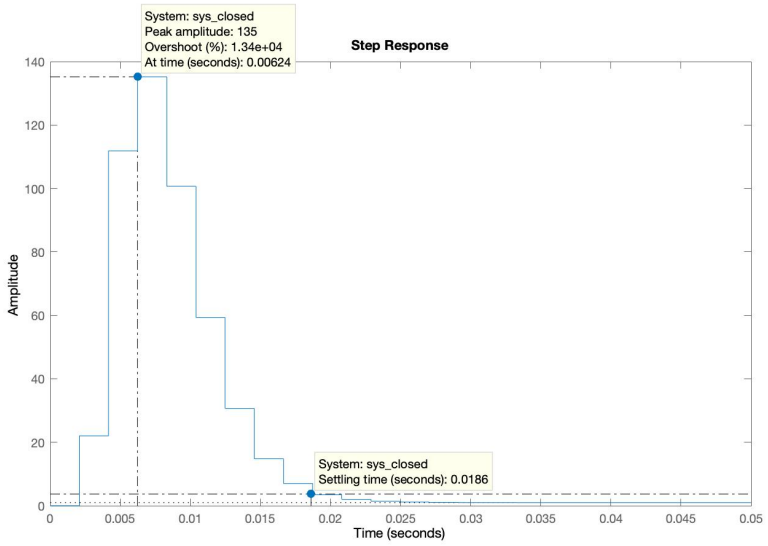

Figure 5.2: Step Response of the system for Set-point step tracking with desired closed loop poles at [0.2, 0.25, 0.3, 0.35]

5.2 Complex system response

The dominant pole rule was here used to simulate the response of the system. In continuous time the dominant poles are solutions of the equation:

$$s^2 + 2\zeta\omega_n s + \omega_n^2 \tag{5.4}$$

where ζ is the damping ratio and ω_n the natural frequency, which determines the speed of convergence. From section 1 the overshoot design objectives is: overshoot $< 5\%$. The following equations which can be used in combination with the design objectives [4].

$$overshoot = 100 \cdot e^{\frac{-\zeta\pi}{\sqrt{1-\zeta^2}}} \rightarrow \zeta = \sqrt{\frac{(ln\frac{overshoot}{100})^2}{\pi^2 + (ln\frac{overshoot}{100})^2}} \tag{5.5}$$

During the design ζ was set equal 0.7 while ω_n was selected so that satisfies $\omega_n = \frac{0.3}{h}$. The continuous time poles were discretized using the zero order hold approximation, which leads to:

$$0 = z^2 + a1z + a2 \tag{5.6}$$

$$a1 = -2e^{\zeta\omega_n h} cos(\omega_n h\sqrt{1-\zeta^2}) \tag{5.7}$$

$$a2 = e^{-2\zeta\omega_n h} \tag{5.8}$$

Finally p_c =[0.35, 0.3, 0.7921+0.1723i, 0.7921-0.1723i]. The system exhibits an overshoot of 6042% and 0.0562 seconds of settling time, as shown in Figure 5.3.

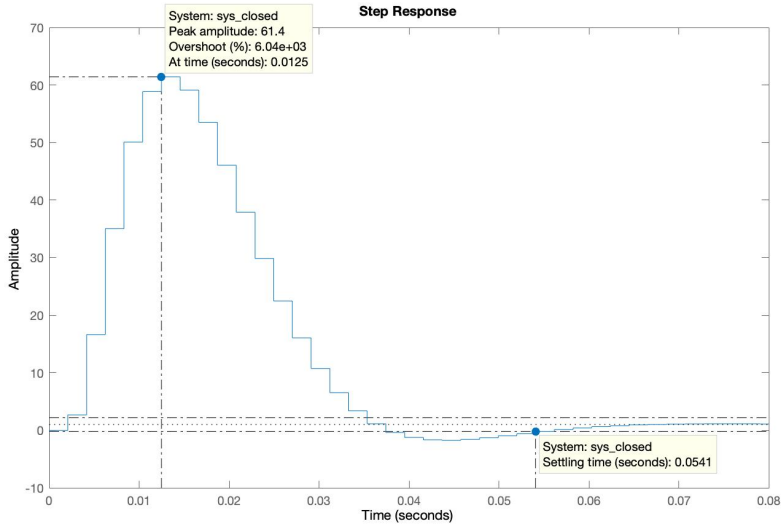

Figure 5.3: Step Response of the system for Set-point step tracking with desired closed complex poles

5.3 Slow system response

The desired closed loop poles were chosen almost near to the unit circle i.e, slower poles were chosen, p_s=[0.8, 0.85, 0.9, 0.95]. Figure 5.4 shows the step response of the system to unit step input as reference. We can see that we have zero overshoot and settling time is 2.09 seconds. The steady state error is also zero and this particular choice of controller meets the control objectives.

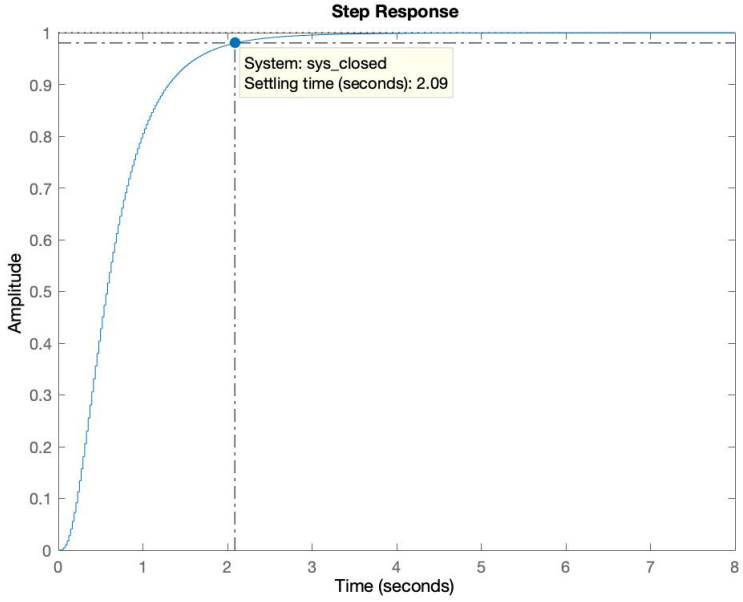

Figure 5.4: Step Response of the system for Set-point step tracking with desired closed loop poles at [0.8, 0.85, 0.9, 0.95]

5.4 Combined system response

Figure 5.5 shows the response of the controller for step reference input. Here we have taken two slower poles (0.9 and 0.95) which are the dominant modes of the system and remaining two poles are the faster poles. As result we have a better performance than the previous section. The overshoot is still zero with settling time of 1.82 seconds. This controller satisfies the design requirements.

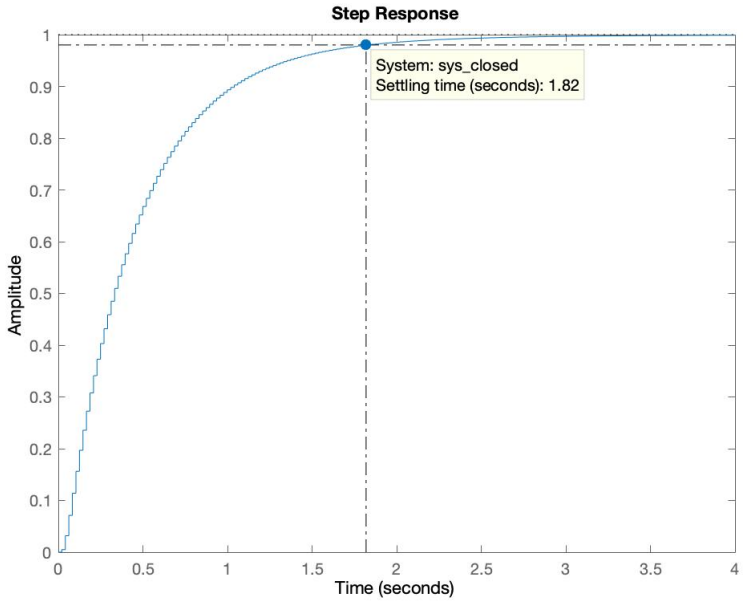

Figure 5.5: Step Response of the system for Set-point step tracking with desired closed loop poles at [0.9, 0.95, 0.2, 0.25]

In this section, we designed the state feedback controller without having any constraints of gain and actuator saturation. As a result we could find multiple closed loop pole locations which would meet the desired control objectives. The effect of location of poles on the magnitude of controller output (plant input) would be discussed in further sections when limits on controller outputs are introduced. The Controller corresponding to the desired poles of [0.2, 0.3, 0.9, 0.95] will be used for design and evaluation of Observer and an Output Feedback Controller in the next section.

6 Discrete Time Output Feedback Controller

In the previous section, a state feedback controller was developed with an assumption that the measurement of states were available. In this section, an Output feedback controller will be developed by adding a dynamic observer to the system which would estimate the states of the system and then be used by the controller (developed in previous section) for feedback. The case of placing slow and fast observer poles are discussed below. The observability matrix of (Φ,Γ) was found to be of full rank and hence the system is observable.
An observer is a linear dynamical system that produces an estimate of the system's state. If we consider the system,

$$x(k+1) = \Phi x(k) + \Gamma u(k), \tag{6.1}$$

we could attempt to determine the state by simply simulating the equations with the correct input, and define the estimate as:

$$\hat{x}(k+1) = \Phi \hat{x}(k) + \Gamma u(k), \tag{6.2}$$

Introducing the error estimation $\tilde{x}(k) = x - \hat{x}$ its dynamics can be described as:

$$\tilde{x}(k+1) = \Phi \tilde{x}(k) \tag{6.3}$$

If Φ has eigenvalues within the unit circle the error will converge to zero. However, the convergence might be slower than desired. Therefore in this section the Luenberger observer will be implemented. Being our system observable we introduce a feedback from the measured output in the form:

$$\hat{x}(k+1) = \Phi \hat{x}(k) + \Gamma u(k) + L(Cx(k) - C\hat{x}(k)) \tag{6.4}$$

The parameter L is called observer gain and through this design the error dynamics become [3]:

$$\tilde{x}(k+1) = (\Phi - LC)\tilde{x}(k). \tag{6.5}$$

Using the separation principle the observer and state feedback gains will be placed separately [2], and the control input is:

$$u(k) = -K\hat{x}(k) + kr * r \tag{6.6}$$

The state space representation of the overall system is:

$$\begin{bmatrix} x(k+1) \\ \hat{x}(k+1) \end{bmatrix} = \begin{bmatrix} \Phi & -\Gamma K \\ LC & \Phi - LC - \Gamma K \end{bmatrix} \begin{bmatrix} x(k) \\ \hat{x}(k) \end{bmatrix} + \begin{bmatrix} \Gamma kr \\ \Gamma kr \end{bmatrix} r \tag{6.7}$$

The sampling period was increased to h=0.06865 seconds, exactly four times smaller that 0.2746 seconds. In few seconds it will appear clear the reason of this choice. The observer poles must be smaller than the poles placed through state feedback. Therefore the state feedback poles introduced previously were converted to continuous time using a zero hold approximation:

$$P_{ct} = \frac{ln(p_d)}{h} \tag{6.8}$$

and set 4 times greater. Finally the inverse conversion was applied finding the discrete observer poles. If the sampling period is too small the observer poles are very close to zero leading almost to the implementation of a "dead bit " observer.

6.1 Slow response and observer

Applying the conversion previously introduced the observer poles for the slow system response result to be p_{os} =[0.8100, 0.9025, 0.6400, 0.7225]. The Matlab command **place(Φ ',Γ ', p_{os})** was used to find the static gain martix of the observer. The response of the system was simulated assuming initial state conditions x(0)=[0.1, 0.1, -0.1, 0.5]'. Figure 6.1 shows the response of the system for a reference step input and the error dynamics. As can be seen from the response, the observer output estimate

converges to the output of the system. The estimates converge in approximately 0.2 seconds and the step response has a settling time of 1 seconds. Comparing the response of this Output Feedback Controller to the responses of Figure 5.2 and 5.3 , we can observe that the overshoot is decreased dramatically but the settling time is increased from 0.05s to 1s due to the unknown initial estimates of the state. This suggests that there is a need for speedy convergence (and hence faster Observer poles) of the observer state estimates to the true states to obtain a Output Feedback Controller which meets the control requirements.

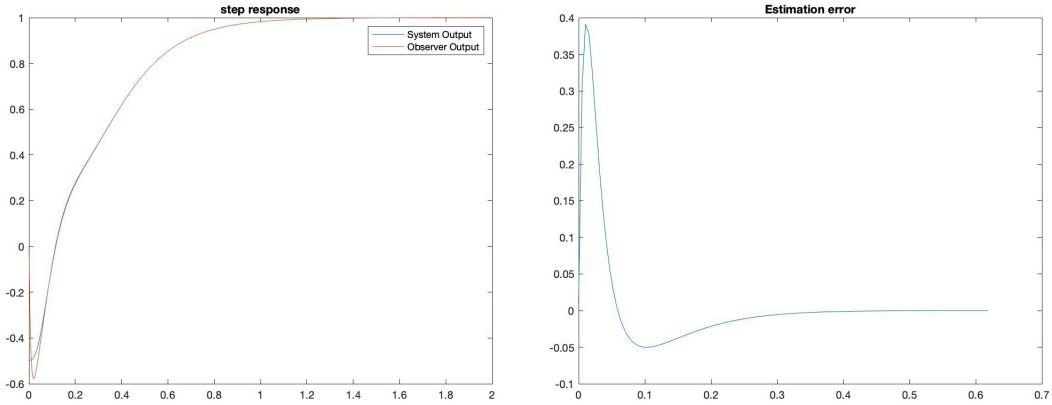

Figure 6.1: Reference set-point step response(left) and error dynamics(right) for slow system

6.2 Fast response and observer

The observer poles placed in this case are faster than the dominant poles of the controller (0.9 and 0.8). The most dominant observer pole 0.65 (-64.07 in continuous time) is 5.8 times faster than the most dominant controller pole 0.95 (-11 in continuous time). Hence all other observer poles are at least 5 times faster than dominant controller poles (0.9, 0.95). The observer poles result to be p_{os} =[0.653, 0.554, 0.133, 0.023]. The response of the system was simulated assuming initial state conditions x(0)=[0.1, 0.1, -0.1, 0.5]'. Figure 6.2 shows the response of the system for a reference step input and the error dynamics. The estimates converge in approximately 0.1 seconds and the step response has a settling time of 0.6 seconds.

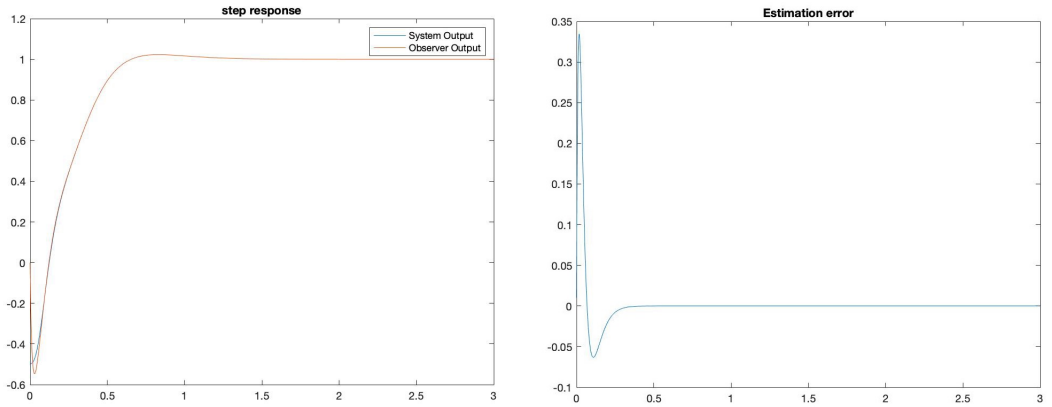

Figure 6.2: Reference set-point step response(left) and error dynamics(right) for fast system

From the Figure 6.2 we can observe that there is a small overshoot. The settling time too has reduced to 0.6 seconds and does meet the control objectives. Comparing this response with the one obtained in Figure 5.5 we can see that the system exhibits a faster response with settling time

decreased from 1.82s to 0.6s. The observer poles can be made much faster, but it would make the system sensitive to measurement noise (which in this case is not considered).

6.3 Input disturbance and observer

In this sub-section it is assumed that an input step disturbance acts on the plant. The state equation in this case is:

$$x(k+1) = \Phi x(k) + \Gamma u(k) + \Gamma\omega, \tag{6.9}$$

Moreover the state is not known but observable therefore again an observer will be implemented. To handle the disturbance an augmented system is defined, which introduces an integral action so in this way the steady state error can be eliminated [4]. Note that the disturbance is not reachable but observable from the output. At the beginning the control input is defined as:

$$u(k) = -K\hat{x}(k) - \hat{\omega} \tag{6.10}$$

to show that the system is able to reject the input disturbance. Later a feed-forward command signal will be added, $k_r r$, proving that the output follows the reference set-point step even in presence of the external perturbation. The control input now becomes as

$$u(k) = -K\hat{x}(k) - \hat{\omega} + k_r r \tag{6.11}$$

The equations of the new state space model of the augmented system are:

$$\begin{aligned}
x(k+1) &= \Phi x(k) + \Gamma u(k) + \Gamma\omega \\
&= \Phi x(k) + \Gamma(k_r r - K\hat{x}(k) - \hat{\omega} + \omega) \\
&= \Phi x(k) - \Gamma K\hat{x}(k) + \Gamma\omega - \Gamma\hat{\omega} + \Gamma k_r r \\
\omega(k+1) &= \omega(k) \\
\hat{x}(k+1) &= \Phi\hat{x}(k) + \Gamma(\hat{\omega} + u(k)) + L_x(y(k) - C\hat{x}(k)) \\
&= \Phi\hat{x}(k) + \Gamma(k_r r - K\hat{x}(k) - \hat{\omega} + \omega) + L_x(Cx(k) - C\hat{x}(k)) \\
&= \Phi x(k) - \Gamma(k_r r - K\hat{x}(k)) + L_x(Cx(k) - C\hat{x}(k)) \\
&= (\Phi - \Gamma K - L_x C)\hat{x}(k) + L_x Cx(k) + \Gamma k_r r \\
\hat{\omega}(k+1) &= \hat{\omega}(k) + L_\omega(y(k) - C\hat{x}(k)
\end{aligned} \tag{6.12}$$

The overall state space system is:

$$\begin{bmatrix} x(k+1) \\ \omega(k+1) \\ \hat{x}(k+1) \\ \hat{\omega}(k+1) \end{bmatrix} = \begin{bmatrix} \Phi & \Gamma & -\Gamma K & -\Gamma \\ 0 & 1 & 0 & 0 \\ L_x C & 0 & \Phi - L_x C - \Gamma K & 0 \\ L_w C & 0 & -L_w C & 1 \end{bmatrix} \begin{bmatrix} x(k) \\ \omega(k) \\ \hat{x}(k) \\ \hat{\omega}(k) \end{bmatrix} + \begin{bmatrix} \Gamma k_r \\ 0 \\ \Gamma k_r \\ 0 \end{bmatrix} r \tag{6.13}$$

As before first the system poles are placed through feedback, after are converted to continuous time and the ones of the observer determined. The system poles are set equal p_s=[0.75 0.65 0.55 0.45], then the observer poles are p_o=[0.5625 0.4225 0.3025 0.2345 0.100], where the last pole was arbitrarily chosen.

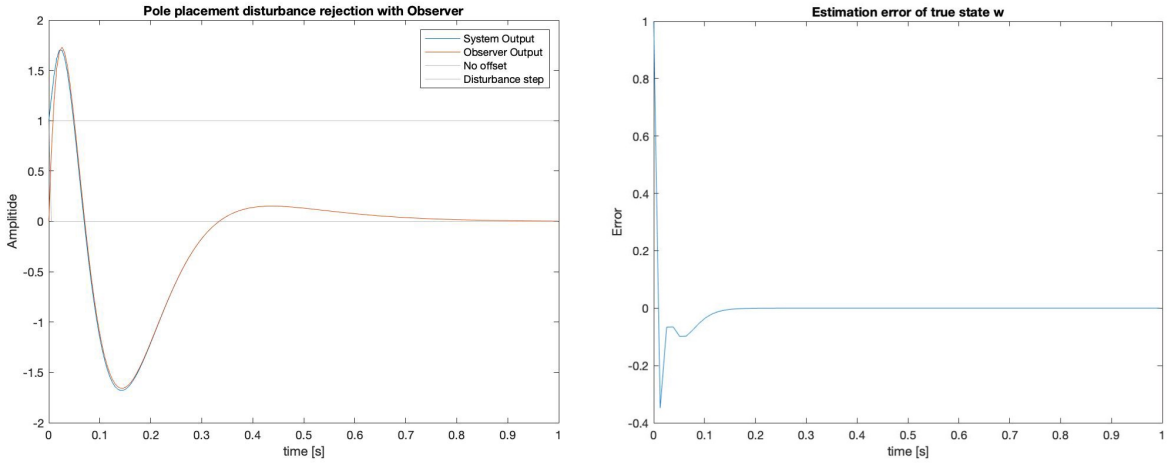

Figure 6.3: Disturbance rejection augmented system with observer(left) and estimation error of the disturbance(right)

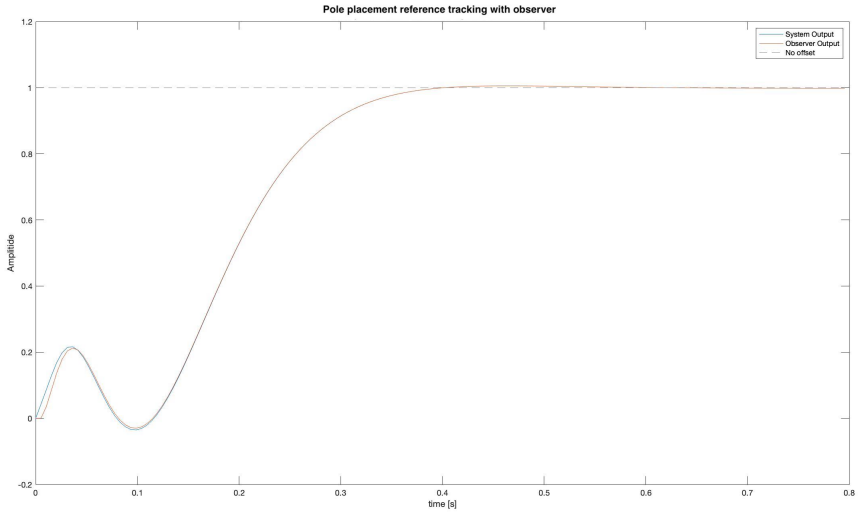

Figure 6.4: Reference tracking augmented system with observer

The step responses of the system for 2 different cases of r_t=0, d_r=1 and r_t=1, d_r=1 are presented, where r_t is the set-point for the tracking and d_r is the load disturbance which acts in the input of the system. Figure 6.3 shows the results of the simulation for the first case with initial value $x_0 = [0\ 0\ \ 0.1\ 1]$. The maximum amplitude reached by the output during the disturbance rejection is ± 1.6. It can clearly be seen that the disturbance ω get estimated over time and there is a correction for that disturbance, which implies that the system accurately follows the reference signal again. Figure 6.4 shows the second reference tracking case with initial value $x_0 = [0\ \ -0.1\ \ -0.1\ 0.1\ 1]$, where settling time is around 0.37 seconds.

Overall, without considering the control effort, the design of the output feedback controller for both reference tracking and disturbance rejection was successful as the controller leads the system to converge to the desired set-point relatively very quickly without large deviations.

7 Linear Quadratic regulator

In this section, a LQ controller is developed with the states of the system estimated by a dynamic Luenberger Observer developed in section 6. In the pole placement method, the desired closed loop poles of the system are specified whose response would meet the required control objectives. An alternate method to develop the linear feedback controller is LQ control.
The linear quadratic regulator problem is one of the most common optimal control problems. Given the linear system:

$$x(k+1) = \Phi x(k) + \Gamma u(k) \tag{7.1}$$

we attempt to minimize the cost function,

$$J_k = min_{uk} \sum_{k=0}^{N-1} \left(x(k)^T Q x(k) + 2x(k)^T Q_{xu} u(k) + u(k)^T R u(k) \right) + x(N)^T Q_0 x(N) \tag{7.2}$$

where the right hand side term is the cost to go with no time left. The parameters to be tuned are the weighing matrix Q and R which would place penalties on states and control input respectively to provide a optimal gain matrix K to minimize the cost function in Equation 7.2. During the design for simplicity Q_{xu} was set equal zero and Q, R diagonal. The Matrix Q is of size n×n where n is the number of states and R is of size m×m where m is the number of inputs. In this case we have Q of size 4×4 and R is a scalar (single input). The diagonal entries in Q place weight on each state individually. It is required that Q is positive semi-definite and R is positive definite matrix.
We start with both Q and R equal to identity. The LQ Controller gains are calculated using the Matlab command **dlqr**. First we discuss the effect of Matrix Q on response of the system to reference unit step input by holding the R constant. The effects of R are then discussed by holding Q constant.

7.1 Constant R = 1 and varying Q

The weighing matrix R was kept constant (identity) and the 4th state i.e the pitch angle of the aircraft was penalized by varying the 4th diagonal element of Q = 1, 100, 1000. Figure 7.1 shows the response of the system to the reference unit step input (left) and the output of the controller (right). By observation, we can see that higher we penalize the states, faster the response and higher the magnitude of the controller output. The different elements of the matrix Q penalizes error in each of the states (with respect to the reference value). Since LQ controller finds the optimal gain to minimize a quadratic cost function, placing higher values in Q would result in faster response reducing rise time and increase overshoot.

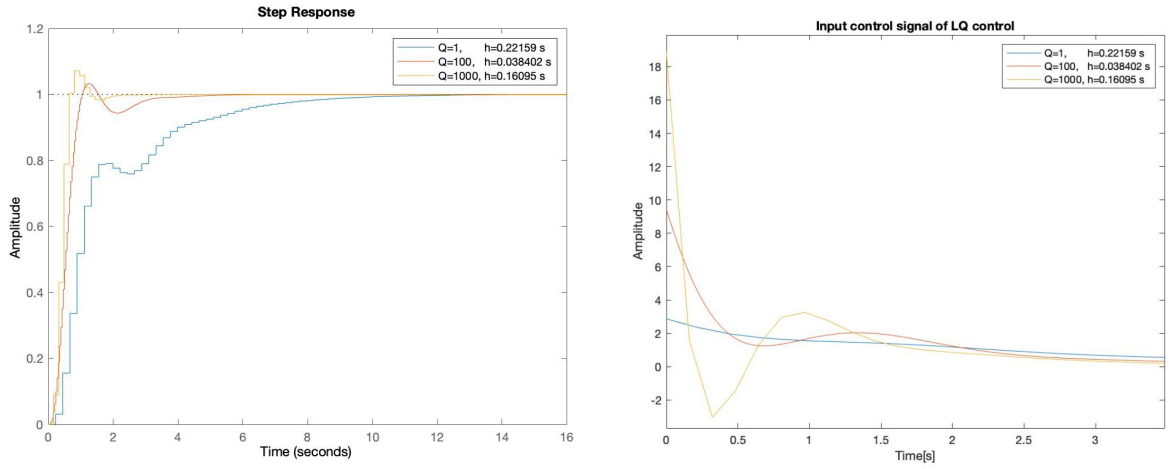

Figure 7.1: Step response of system (left) and control effort (right) for varying Q and R = 1

7.2 Constant Q= diag(1,1,100,1000) and varying R

Now the Matrix Q was made constant and the controller output was penalized by varying R = 0.01, 1, 100. Figure 7.2 shows the the step response of the system and controller output. Less the value of R, less penalty is placed on controller output and hence the magnitude of the control action can be quiet large. As a result, the response of the system is fast. As the value of R is increased, optimal gain matrix K is constructed in such a way that reduces the magnitude of the resulting control action. The response of the system is hence slower. Selecting appropriate weighing matrices Q and R is a trade off between response time of the system and resulting magnitude of the control action.

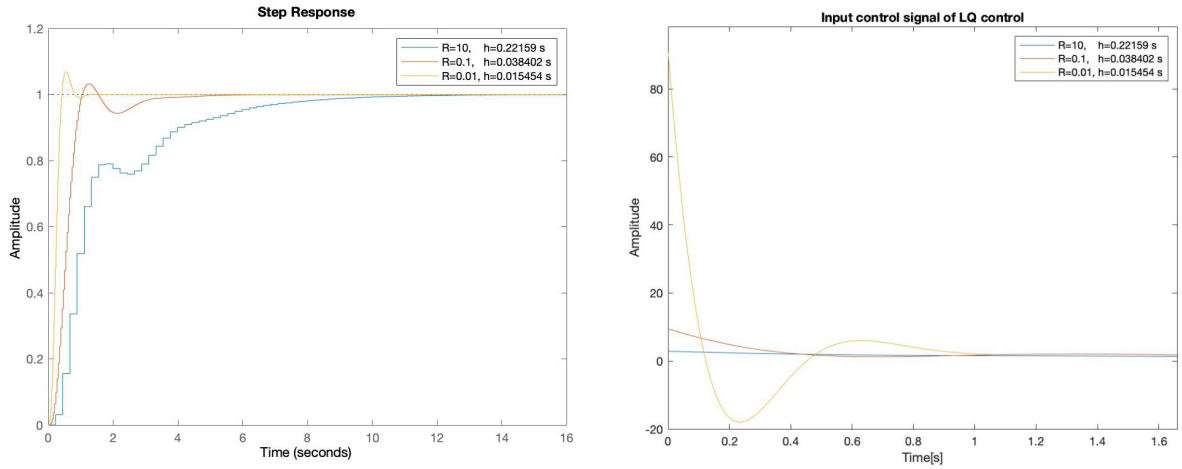

Figure 7.2: Step response of system and control effort for varying R and Q=diag(1,1,100,1000)

7.3 Final designed LQ Controller

Now that the influence of Q and R on the response of the system have been discussed, a LQ controller that meets the control objectives is developed by tuning the Q and R matrices. Figure 7.3 shows the response of the system for reference step input. Settling time is 2.63 seconds with a overshoot of 4.62%. The system starts to become marginally stable and more oscillations start to occur, this can be seen in the step response. The Q matrix used to obtain this response is Q = diag(1,1,100,100). High penalty was placed on angular position to obtain a faster response and penalty of 100 was placed on angluar velocity (3rd state) which acts like damper to reduce the overshoot. Low penalty of R = 0.01 was placed on control action to achieve fast response.

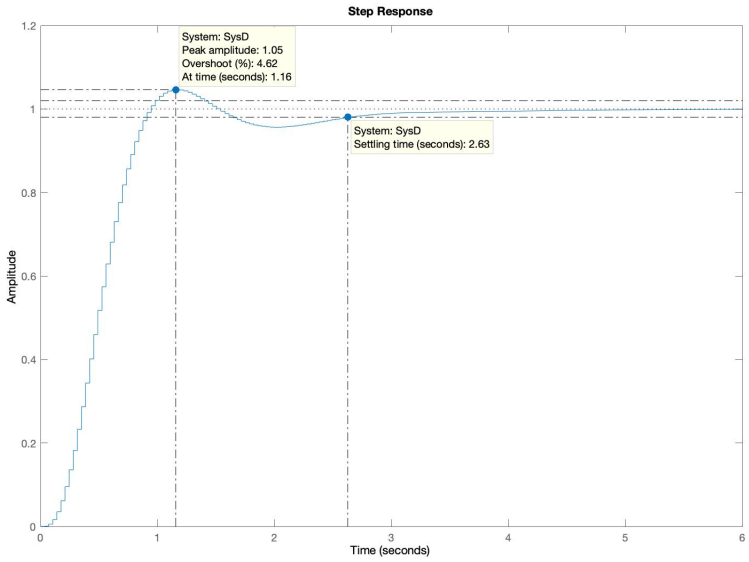

Figure 7.3: Step response of system for R=0.01 and Q=diag(1,1,100,100), h=0.0259 s

Until now, no limitations were placed on the magnitude of controller output and controllers were designed without taking the effects of actuator saturation in to account. In the following sections, the controller outputs of the controllers are examined and effects of actuator saturation are discussed. The effect of sampling period is also discussed.

8 Control Action

In this section we examine the controller output of all the controllers designed in previous sections and impose limitations on the controller outputs. The controllers are then re-tuned to avoid saturation in section 9, 10 and 11.
In the following figures the control action for the different controllers are shown. It can be seen that for most controllers they start of with an extremely high control action and then start to tend towards zero. It is clear that this is well above the ±5. The exception is the PID disturbance rejection controller which is remarkably low in comparison to the rest and is even under the ±1.5 mark.

8.1 Control action generated by Discrete controllers

Figure 8.1 shows the output of the controller developed in section 4 for set-point tracking(left) and disturbance rejection(right).

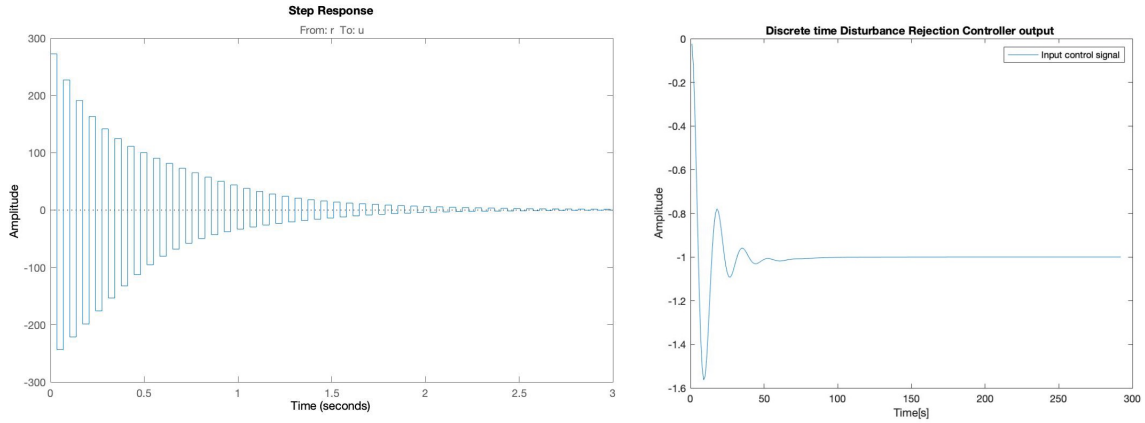

Figure 8.1: Discrete time set-point tracking(left) and disturbance rejection(right) controller output

The maximum amplitude of the control signal for tracking of a reference step input is approximately ±280 (with settling time of approximately 2.34 seconds), which is a very huge value and can easily saturate the actuators. The maximum amplitude of the controller output for a unit step disturbance at the plant input is around -1.5.

8.2 Pole placement observer controller output

Figure 8.2 shows the controller outputs of four Pole Placement Observer systems for set-point tracking discussed in section 5. Having faster poles as the poles of closed loop system to achieve fast response has resulted in high magnitude of control signal. The magnitude of the controller output for set-point tracking in this case is within the limits $\pm 1.5 * 10^9$.

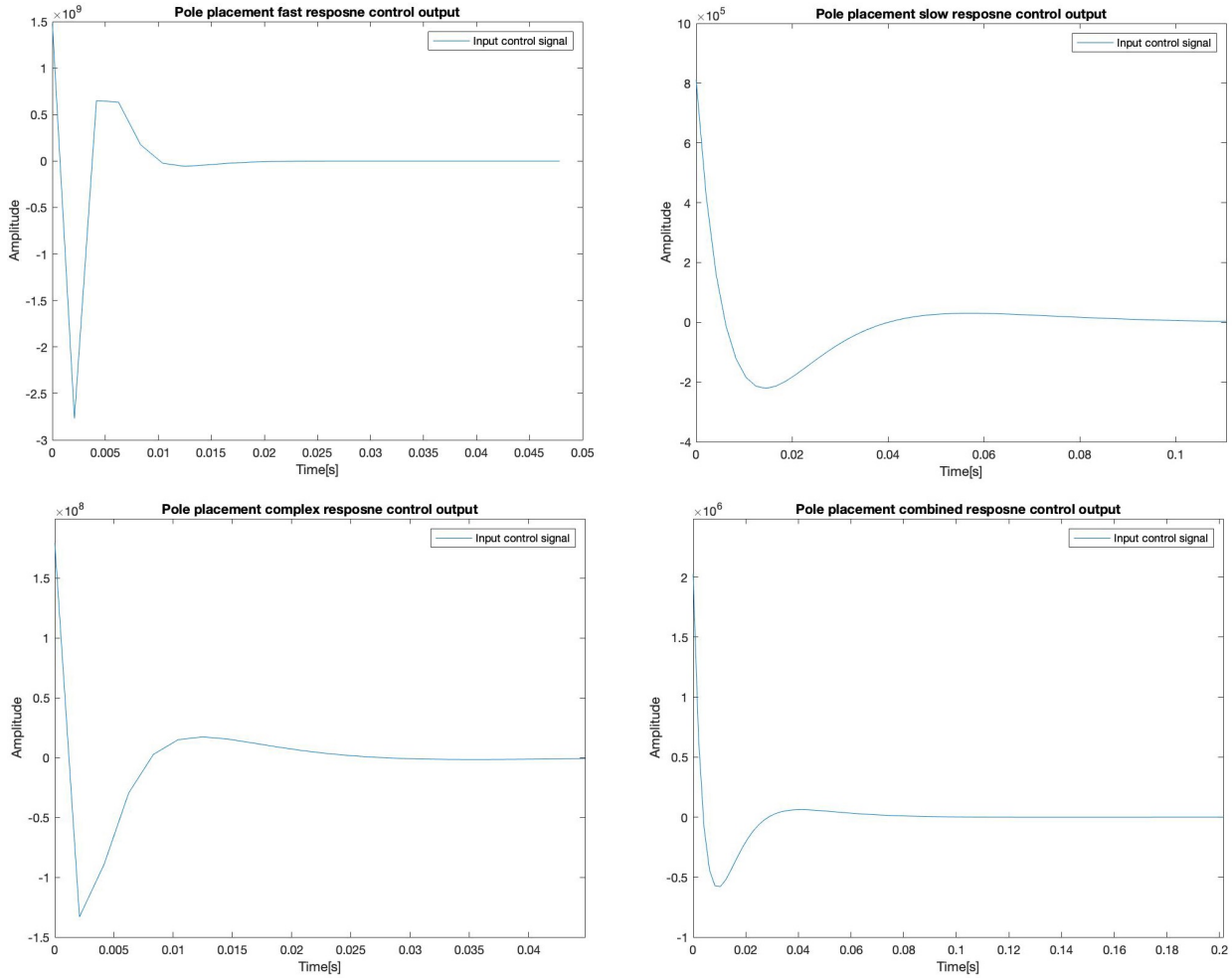

Figure 8.2: State Feedback set-point tracking controller outputs

8.3 Output Feedback Controller output

Figure 8.3 shows the controller outputs for set-point tracking and disturbance rejection. Magnitude of the control signal is higher in this case for disturbance rejection.

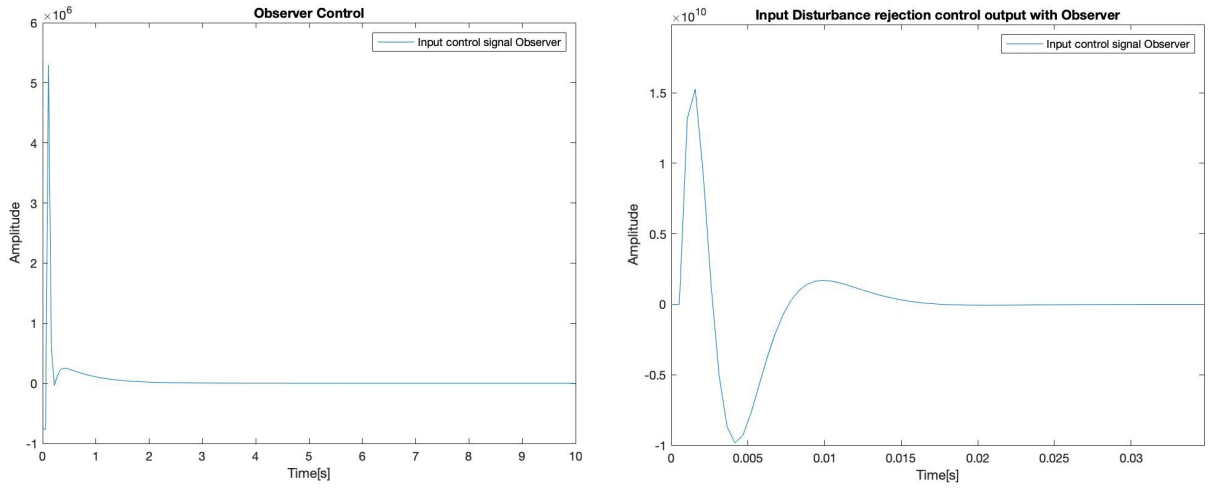

Figure 8.3: Output Feedback controller output

8.4 LQ Controller Output

Figure 8.4 shows the control signals generated by the Final LQ controller discussed in section 7.3. Here the magnitude of the control signal for set-point tracking is way lower than the previous controllers and within limits ±10. However the settling time in this case was 3 seconds. This is due to the nature of the LQ controller which optimizes the performance by considering the trade-off between the magnitude of control signal and deviation in the states through R and Q matrices respectively.

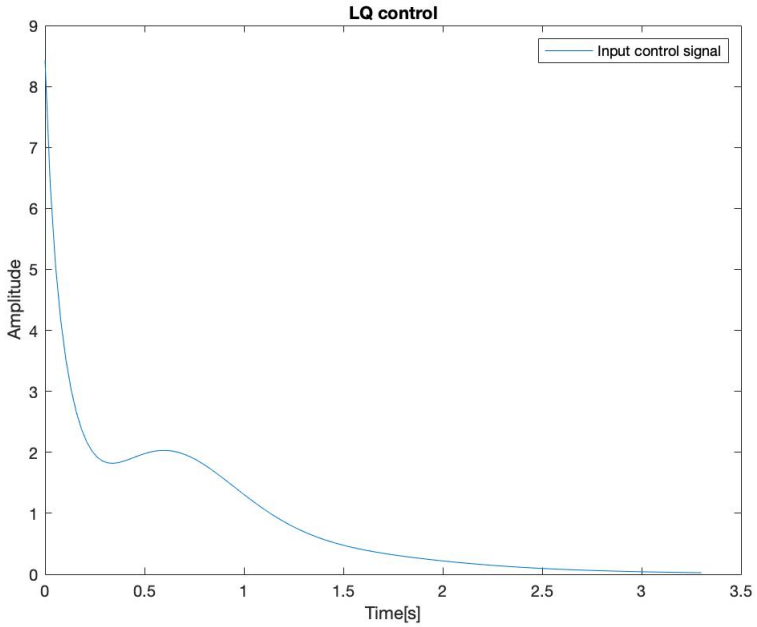

Figure 8.4: LQ controller set-point tracking output

Clearly, in all the controllers designed, we are trying to achieve a faster response resulting in larger magnitudes of control action. We did not take into account the limitations on controller output to avoid actuator saturation. By limiting the controller output to a value of ±5, we need to re-tune the controllers to avoid actuator saturation and still be able to achieve the control objective. Here the trade off between the magnitude of the control signal and the response time needs to be made among all the controller designs. Section 9 discusses the controllers designed in section 4 with actuator saturation. Section 10 revisits the Pole placement controller and in section 11 we tune the parameters Q and R to obtain a LQ controller which avoids actuator saturation.

9 PID Redesign

In section 8, it was seen that the magnitude of control signal was quite large for tracking of reference step input. Hence the controller need to be changed to avoid saturation of actuator. For the redesign of the PID controllers only the the tracking controller needs to be redesigned because for the case of disturbance rejection the PID controller designed in section 4 does not exceed the limit.
In order to limit the output of the controller to ±5, we reduce the crossover frequency of PD Controller designed in Section 1, which will reduce the gain and appropriately shift the phase lead with it. The redesigned PD Controller in continuous time domain is shown below in Equation 9.1,

$$C_{pd} = \frac{4.3937(s+10)}{(s+20)} \tag{9.1}$$

The PD Controller is discretized using Matlab command **c2d** with a sampling period of h = 0.082s. The transfer function of the discretized PD Controller is illustrated in Equation 9.2.

$$C_{pd} = \frac{3.4087(z-0.422)}{(z-0.1032)} \tag{9.2}$$

In Figure 9.1, the bode plot of redesigned system has crossover frequency = 0.384 rad/s. Figure 9.2 shows the step response of the system for PD Controller.

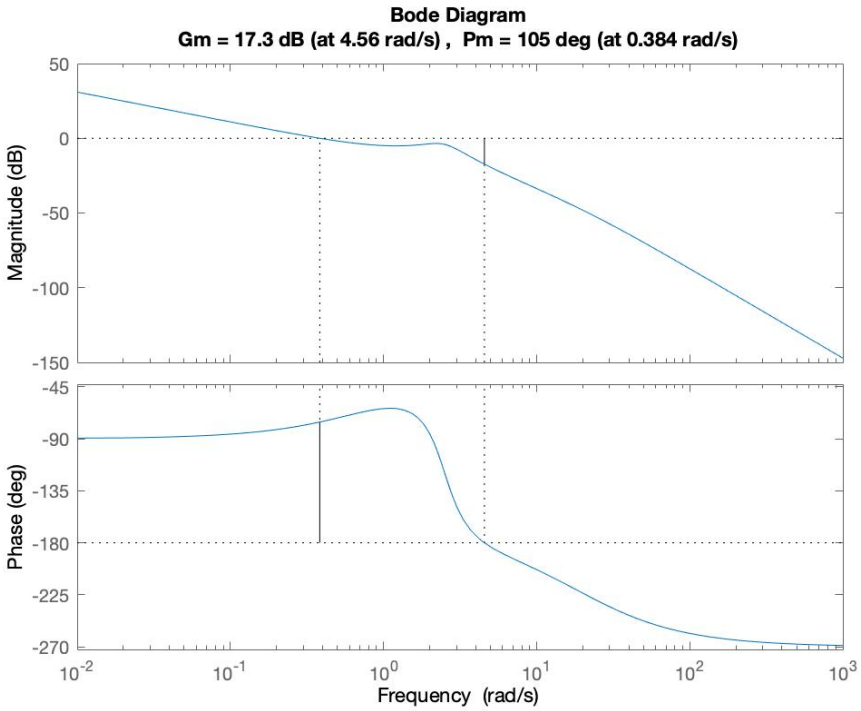

Figure 9.1: Bode plot of the open loop system with redesigned controller

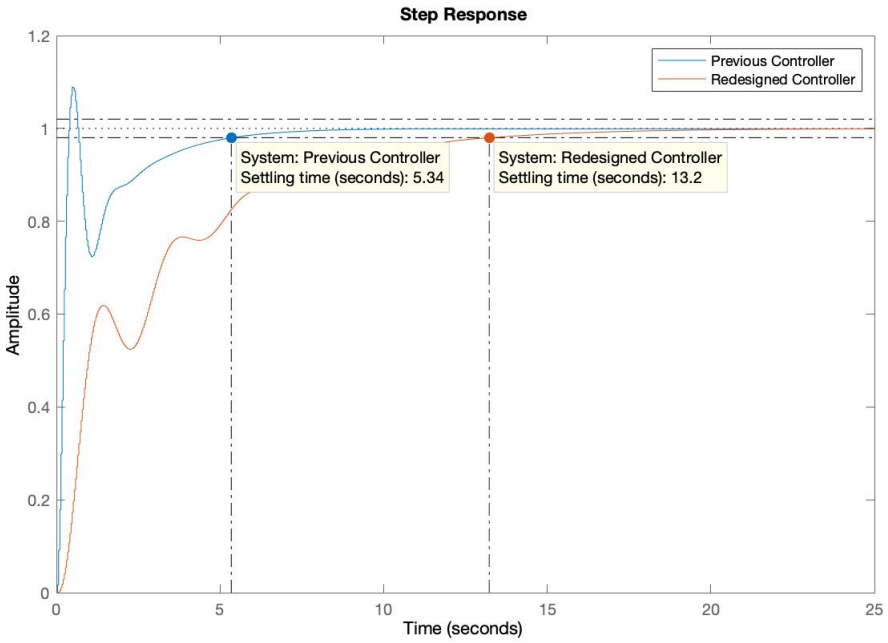

Figure 9.2: Step response comparison between previous and redesigned Controllers

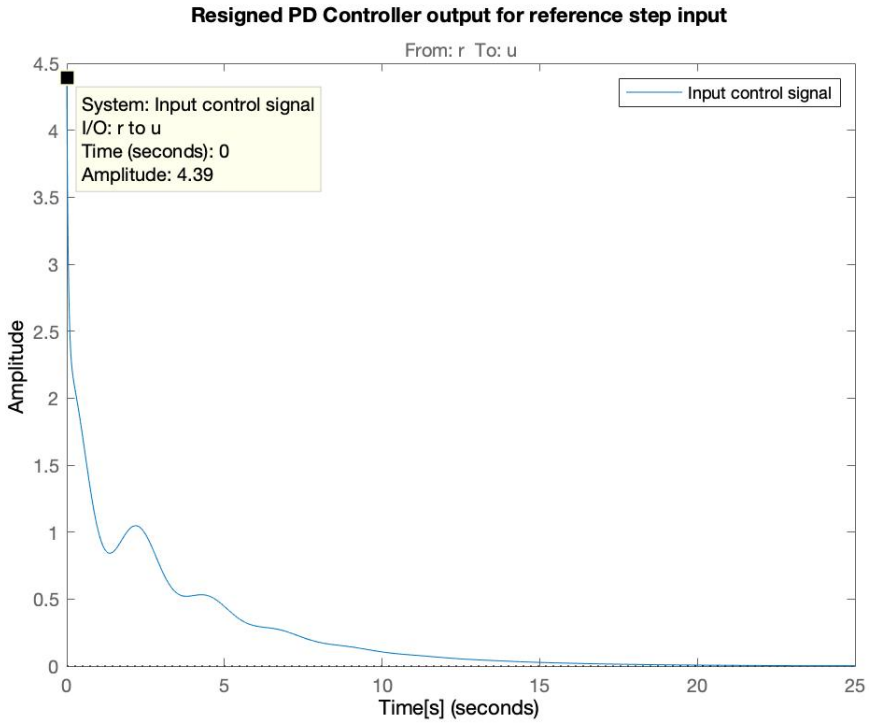

Figure 9.3: Controller effort of redesigned Controller

It can be seen that the settling time is 13.2 secs and no overshoot. From Figure 9.3 it can be seen that the controller output is within limits to avoid saturation of actuator. Here in order to reduce the magnitude of control signal the response time was traded off.

10 Pole Placement Redesign

In section 8 it was seen that the output of the controller was beyond the limits of ±5. In order to avoid the saturation of actuator, the slow poles were chosen as the desired closed loop poles. Earlier the desired closed loop poles were [0.2, 0.25, 0.9, 0.95]. The new closed loop poles were chosen as [0.992, 0.993, 0.994, 0.995]. The new sampling time is 0.01s. The numbers up to three decimal places were considered because the sampling interval of 0.01 was too small and higher decimal places become important when dealing with small sampling instants. Figure 10.2 shows the response of the system for tracking reference step input and Figure 10.1 shows the control action generated by the controller.

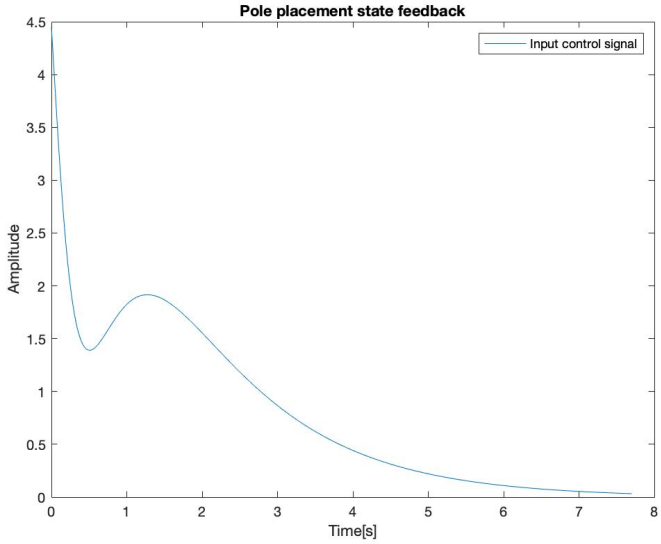

Figure 10.1: Controller effort of Pole Placement State Feedback Controller for reference tracking

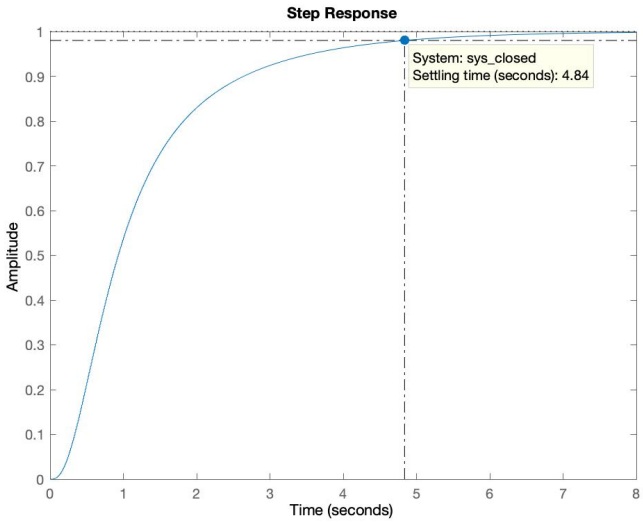

Figure 10.2: Step response of State Feedback Controller

It can be seen that the response time (settling time of approximately 4.84 seconds) has been compromised to keep the control signal within limits, which however is 4 times as fast as the settling time achieved in section 9.

11 LQ Control Redesign

With the LQ method the Q and R matrices can be used to emphasize the cost of the states or the cost of the control input. Because the control input needs to be reduced the R matrix which emphasizes the cost of control was increased until the cost of control was reduced to ±5. This gave the following result

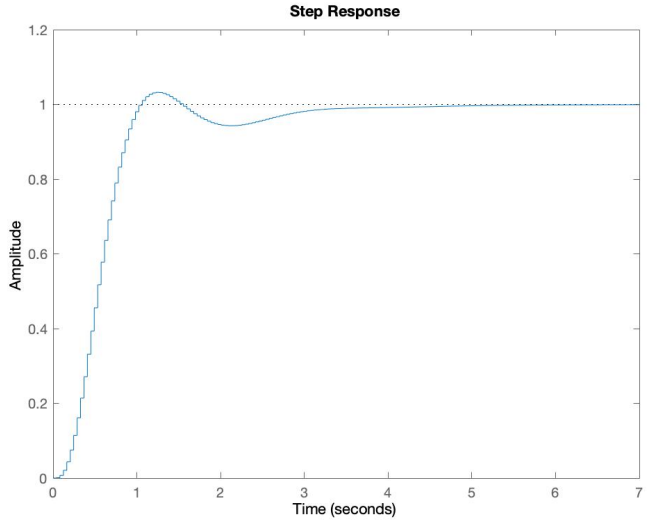

Figure 11.1: Step response of LQ Controller with Q=diag(1,1,10,10) and R=10

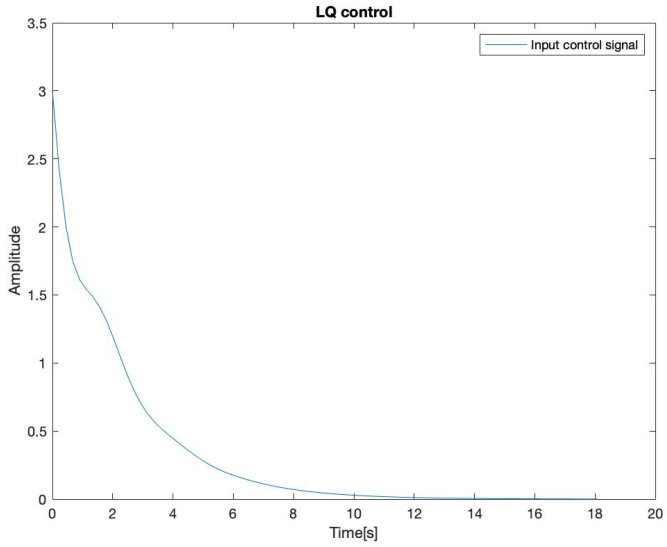

Figure 11.2: Controller effort of LQ Controller for reference tracking

From Figure 11.1 we can see a nice step response with 3.67% overshoot and it almost uses the maximum control input as shown in Figure 11.2. It is faster than the pole placement and gives better results than the PID control. Also the emphasize on the control input is a lot bigger than the ideal case as proposed to solve the problem. Another angle of approach could be to reduce the emphasize on the states so they don not need to be reduced as fast as possible because they cost so much and thus a weaker control signal can be used to satisfy the cost function.
Similar to section 9, the LQ Controller was evaluated for step disturbance input at plant input. Figure 11.3 shows the response of the system for disturbance input. In this case, we can see a offset induced

by the disturbance. Section 12 provides a solution to get rid of the off/steady state error.

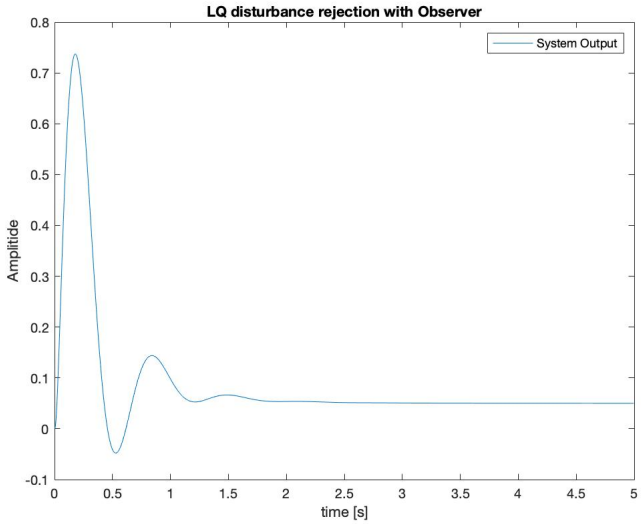

Figure 11.3: Response of system for disturbance rejection using LQ Controller

12 Dealing with steady state errors

In section 11, it was seen that the steady state error becomes significant for a step disturbance at plant input when there is a controller output limitation. To completely remove this offset an integrator was added which integrates the error between the output and the reference and provides it as control input to the plant in addition to existing LQ controller.
The basic approach in integral feedback is to create a state within the controller that computes the integral of the error signal, which is then used as a feedback term. For the case of output feedback controller in question 6, it was shown that by the addition of disturbance observer which was acting like an integrator, the steady state error converges to zero again even in the presence of step set-point and step disturbance. Thus, in this section, we do this by augmenting the description of the system with a new state z:

$$\begin{bmatrix} x(k+1) \\ z(k+1) \end{bmatrix} = \begin{bmatrix} \Phi & 0 \\ C & 0 \end{bmatrix} \begin{bmatrix} x(k) \\ z(k) \end{bmatrix} + \begin{bmatrix} \Gamma u(k) \\ -r \end{bmatrix} \tag{12.1}$$

The state z is seen to be the integral of the difference between the the actual output y and desired output r. If we find a controller that stabilizes the system, then we will necessarily have z=0 in steady state and hence $y = r$ in steady state. Given the augmented system, we design a state space controller, with a control law of the form:

$$u(k) = -Kx(k) + k_i z(k) + kr * r \tag{12.2}$$

where K is the usual state feedback term, k_i is the integral term and kr, equal one over the zero frequency gain, is used to set the nominal input for the desired steady state.
Using this controller the system response was simulated for step disturbance input of magnitude of 0.1 acting at plant input. Figure 12.1 shows that the addition of integrator is able to remove the steady state error in LQ Controller (left) while the control signal generated is within the limits (right).

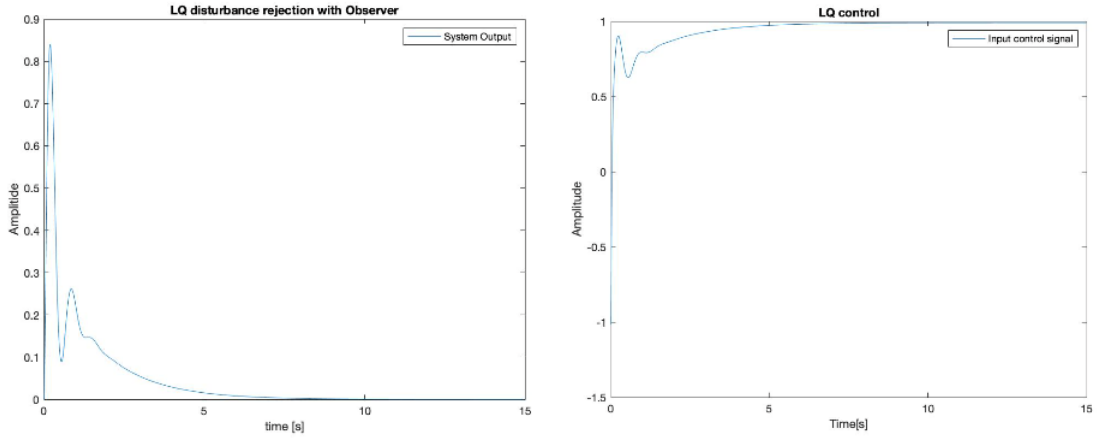

Figure 12.1: Output of system for step disturbance input (left) and Controller output for LQ Controller with integrator

13 Input Delay

In this last section one time step input delay will be introduced in the controllers implemented in previous sections.
Typically, one extra time step delay is introduced by the computation of the control algorithm. As the reader may understand this could destabilize the system or deteriorate the performances, the controller is one step below the dynamics of the plant. It is required therefore to model the one sample time delay.
Under this conditions our general state space equation will be:

$$x(k+1) = \Phi x(k) + \Gamma u(k-1) \tag{13.1}$$

$$y(k) = Cx(k) \tag{13.2}$$

To compensate the delay we introduce a shift register, augmenting our system in the form [3]:

$$\begin{bmatrix} x(k+1) \\ u(k) \end{bmatrix} = \begin{bmatrix} \Phi & \Gamma \\ 0 & 0 \end{bmatrix} \begin{bmatrix} x(k) \\ u(k-1) \end{bmatrix} + \begin{bmatrix} 0 \\ 1 \end{bmatrix} u(k) \tag{13.3}$$

As will be demonstrated in the following pages through this new state space representation is possible to implement a controller so that the design objectives are satisfied.
However, before moving to that at the beginning the extra time delay will be incorporated in the PID type controller previously implemented, and if required these will be redesigned. If we take the z transform of Equation 13.1, assuming initial conditions x(0)=0 we obtain:

$$zX(z) = \Phi X(z) - \Gamma z^{-1} U(z) \tag{13.4}$$

$$X(z) = (zI - \Phi)^{-1} \Gamma z^{-1} U(z) \tag{13.5}$$

$$Y(z) = C(zI - \Phi)^{-1} \Gamma z^{-1} U(z) \tag{13.6}$$

The controller transfer function is pre-multiplied by the inverse of the complex variable z [2].

13.1 PID Controllers

In this question the discrete transfer functions were used because it's easier to add an delay to those. They are computed as was described in the note from Section 4. For the discrete time transfer functions only a z^{-1} operator should be added to achieve the time delay. This would change the controller in to

$$C(z) \to C(z)z^{-1} \tag{13.7}$$

for the tracking controller this gave the following performance of the step input.
Clearly a deterioration in the performance can be seen in Figure 13.1, the system displays high overshoot of 16.4% and is more oscillatory. This can be explained by the drop of phase lead which reduces the damping in the system. It was required therefore to redesign the controller increasing the phase margin. The response of the system to a step input with the augmented shift register is shown in Figure 13.2, which assures a phase margin of about 63 degrees. The overshoot was reduced to 2.23% satisfying the design objectives. The parameter information of the original PD controller and redesigned PD controller are provided in Table 13.1.

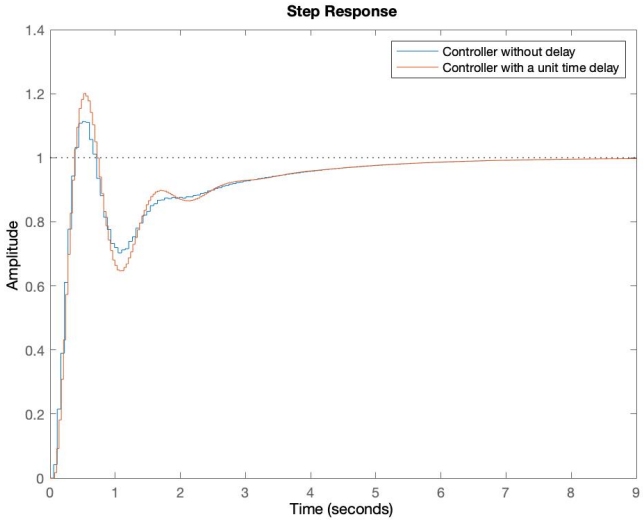

Figure 13.1: Step response PD tracker without (blue) and with (red) time delay

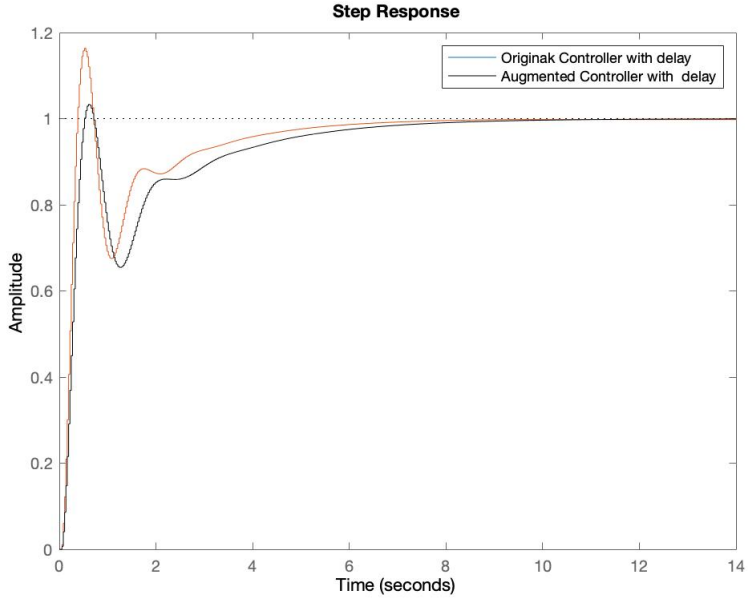

Figure 13.2: Step response of original PD Controller (red) and Augmented Controller (black) both with time delay

The transfer function of the system for the disturbance rejection case is:

$$Y(z) = \frac{zG(z)}{z + G(z)C(z)}Q(z) \tag{13.8}$$

As before the extra delay introduces a phase lag in the system, the phase margin decreases to almost 30 degrees. As shown in Figure 13.3, for the case of PID controller which is designed for disturbance rejection, the maximum amplitude of the response is increased from 0.018 to 0.023 while the settling time is also increased from 2.73 sec to 7.87 sec. Undoubtedly the influence of the one time step delay to the time domain performance characteristics of the PID controller is not very significant as the deviation from the initial design requirements is not very large, but the controller should be redesigned in order to satisfy the design criteria. Figure 13.4shows the redesigned PID controller for disturbance rejection input delay. The parameter values of the original PID controller and the redesigned PID

controller are collected in Table 13.1.

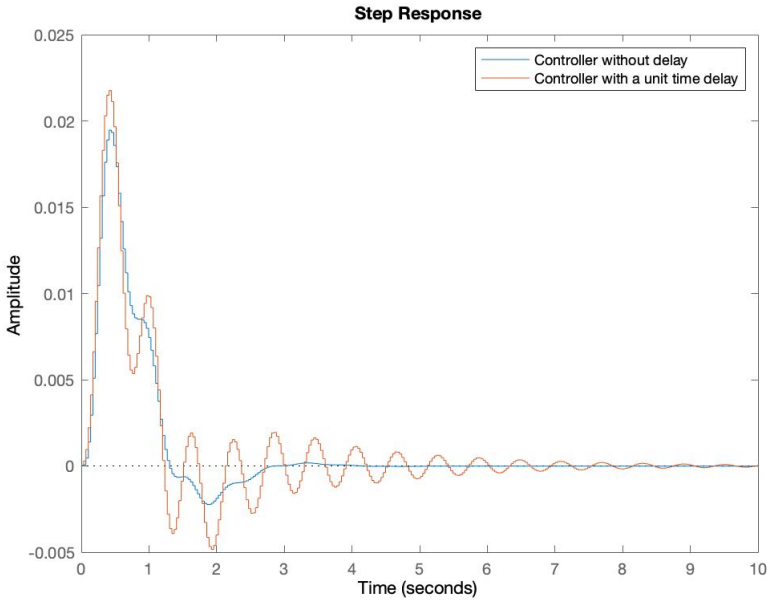

Figure 13.3: Step response PID disturbance rejector without (blue) and with (red) time delay

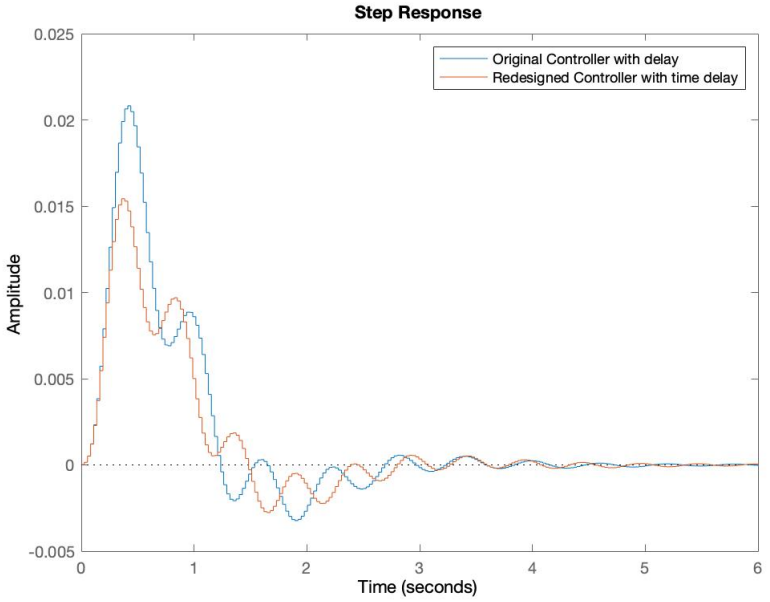

Figure 13.4: Step response original PID disturbance rejector (blue) and redesigned PID rejector (red) both with time delay

Table 13.1: Performance characteristics of original and re-designed PID controllers

name	A_p	T_d	η	PM(deg)	ω_c(rad/s)	GM	P.O(%)	S.T(s)	
original(PD)	9.3	0.5	100	50.3	5.36	51.3	16.4	5.32	
redesigned(PD)	6.5	0.4	40	51	4.05	30.3	2.37	6.4	
name	K_p	T_i	T_d	N	PM(deg)	ω_c(rad/s)	GM	M.A	M.D.D(s)
original(PID)	40	0.4	0.35	35	25.1	10.3	15.1	0.0208	3.54
redesigned(PID)	50	0.4	0.37	80	25.8	12.1	19.4	0.0154	3.51

13.2 Pole Placement

For the pole placement controller, with extremely fast response, adding a time delay could be detrimental for the reference tracking. It can clearly be seen that the system has become unstable, the old system isn't even visible in the Figure 13.5. The reason it has become unstable is because the extremely fast response of the system causes the discrete poles to be pushed to the edge of the unit circle. Adding 'instability' by introducing phase lag pushed this system over the edge and made it unstable.

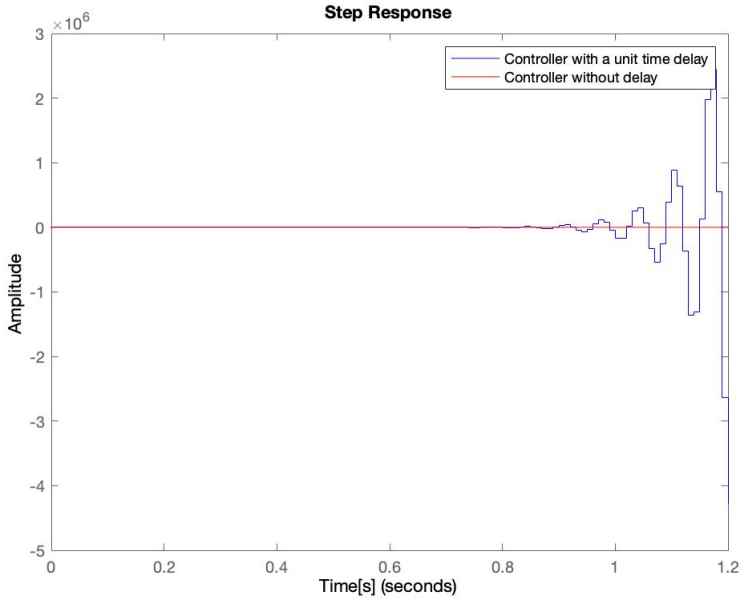

Figure 13.5: The pole placement controller without and with time delay

While during the PID type controllers design to compensate the delay input was required to increase the phase margin of the system, during the pole placement tuning an additional pole will be included. Defining the new augmented state as $z(k) = [x(k), u(k-1)]'$, our controller is:

$$u(k) = -K_z z(k) + kr * r \tag{13.9}$$

Using this control law Equation 13.3 can be written as:

$$\begin{bmatrix} x(k+1) \\ u(k) \end{bmatrix} = \begin{bmatrix} \Phi & \Gamma \\ -k_x & -k_u \end{bmatrix} \begin{bmatrix} x(k) \\ u(k-1) \end{bmatrix} + \begin{bmatrix} 0 \\ kr \end{bmatrix} r \tag{13.10}$$

where k_x is a row vector of dimension 1x4 and k_u a scalar [1]. The state space system as done in section 5 was discretized using the zero order hold approximation and a sampling period of 0.019286 seconds. The poles location was chosen to be p_d =[0.95, 0.85, 0.4, 0.45, 0.3]. The step response of the

redesigned pole placement controller with time delay is shown in Figure 13.6.There is no overshoot or steady- error and the settling time is 2.164 seconds.

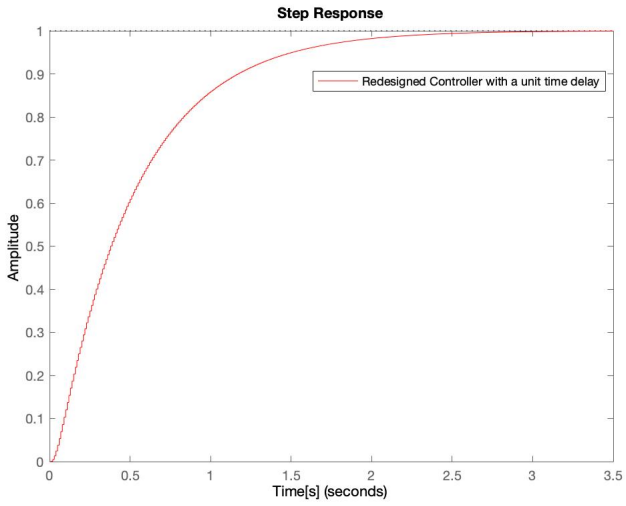

Figure 13.6: The redesigned pole placement controller with time delay

13.3 Observer with disturbance

For the output feedback controller with input disturbance, since sampling time of 0.03 seconds was very small, the delay made no significant effect on the performance of the controllers. In order to understand the effects of the delay, the sampling period was increased to 0.1 seconds and the output feedback controller developed in section 6 was simulated. Adding a time delay renders the step response of disturbance rejection unstable as shown in Figure 13.7.

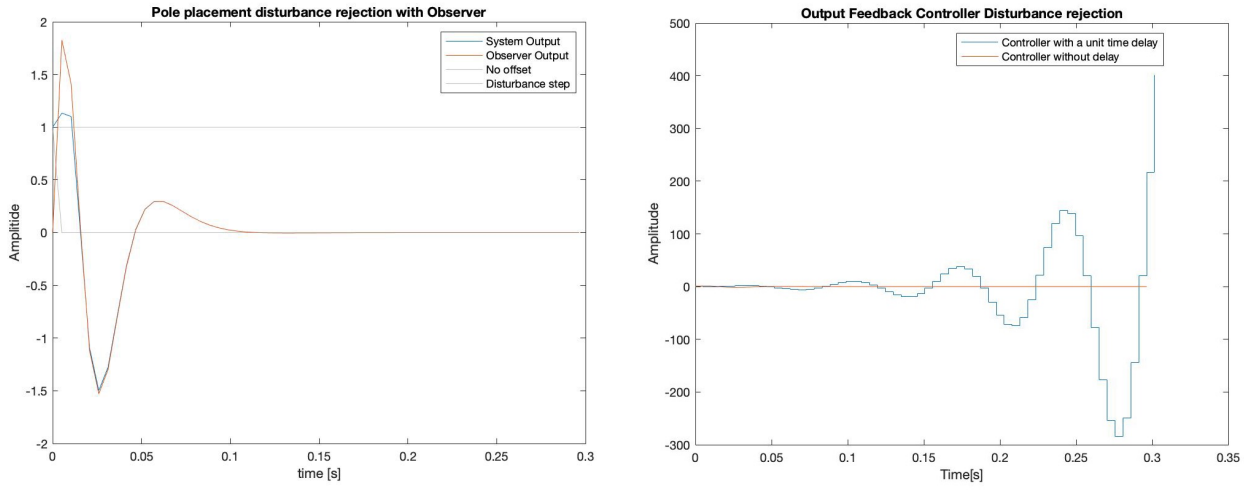

Figure 13.7: Observer with disturbance rejection without (left) and with (right) time delay

It can be seen that the system exhibits a very different performance than expected. In the following the output feedback controller was re-tuned to achieve the required control performance by augmenting the state space model with the delayed input. Meanwhile, two additional states are introduced, one for the disturbance and one for it's estimate. Including also the delayed input state, the state space of the augment system becomes now:

$$\begin{bmatrix} x(k+1) \\ \omega(k+1) \\ \hat{x}(k+1) \\ \hat{\omega}(k+1) \\ u(k) \end{bmatrix} = \begin{bmatrix} \Phi & \Gamma & \Gamma & 0 & 0 \\ 0 & 0 & 1 & 0 & 0 \\ L_x C & \Gamma & 0 & \Phi - L_x C & \Gamma \\ L_w C & 0 & 0 & -L_w C & 1 \\ 0 & -1 & 0 & -K & 1 \end{bmatrix} \begin{bmatrix} x(k) \\ \omega(k) \\ \hat{x}(k) \\ \hat{\omega}(k) \\ u(k-1) \end{bmatrix} + \begin{bmatrix} 0 \\ kr \\ 0 \\ 0 \\ 0 \end{bmatrix} r \tag{13.11}$$

with the input signal is given as:

$$u(k) = kr * r - K\hat{x}(k) - u(k-1) - \hat{\omega}(k) \tag{13.12}$$

The feedback poles are p_f=[0.9 0.95 0.4 0.23 0.1], while the observer poles p_o=[0.8463 0.9023 0.1296 0.0841 0.1000]. Figure 13.8 shows the response of the system to a unit step disturbance, we can see that the controller is able to reject the disturbances and the control signal generated is also within the specified limits.

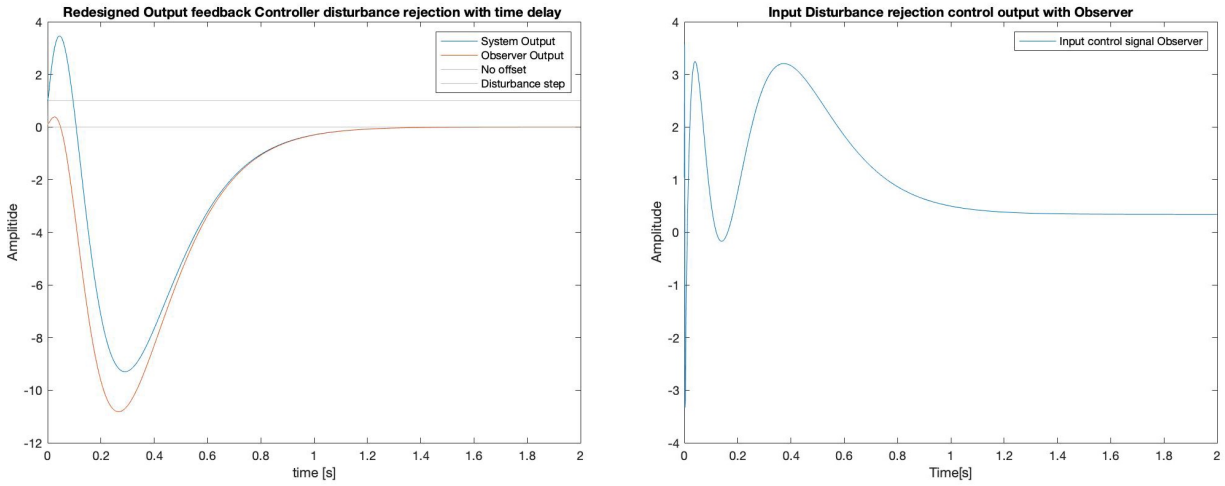

Figure 13.8: Response of the redesigned output feedback controller with time delay for disturbance rejection (left) and control effort (right) of the controller

13.4 LQ Controller

The LQ control with a single time delay shows the following step response as shown in Figure 13.9.

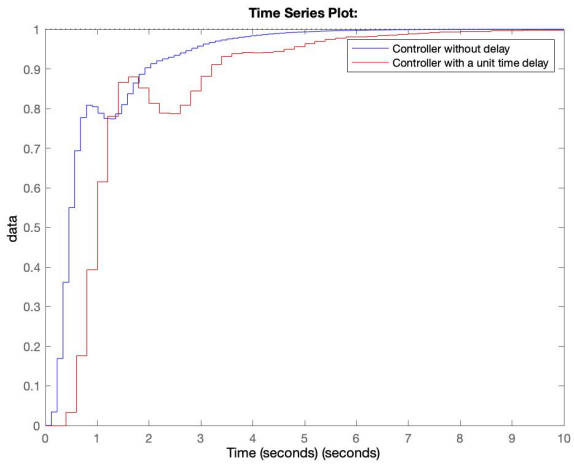

Figure 13.9: Linear Quadratic regulator input delay

Clearly the delayed system shows some performance deterioration but very little. We know from continuous time that the LQ controller has amazing stability properties. This is showcased here in discrete time with a fast respond even though there is a time delay. The LQ controller has no problems, so there is nothing that needs to be redesigned.

14 Conclusion

In this assignment, various control algorithms were developed in a supersonic jet pitch angle position system, employing tools from Continuous and Discrete Time Control system theory.

Based on our observation, the supersonic control system can be accelerated to react vert fast, even considering the control action limitations. The LQ Controller yields the best results considering the control output limitations, with the smallest settling time of (2.67 seconds) compared to Pole-Placement controller of (4.84 seconds) and PID controller (13.10 seconds), and behaves the amazing stability properties with time delay. The Pole-Placement Controller comes to second because of the flexibility of placing poles for achieving different speed of system response. Output Feedback Controller can estimate and compensate the input disturbance if the information about the nature of the disturbance is available, if this is not the case it can be tricky. Lastly, PID controller designing is sensitive to the control effort limitations and time delay, and is difficult to be tuned perfectly compared to LQ Controller.

The difference of the system responses between the case when there are no control action limitations and when we deal with actuators saturation should be emphasised in the end. In a real supersonic jet pitch angular systems, the controller output magnitude is not within ± 5 and the system operating frequency is not 1 Hz, as in the control reduction section. However, the results presented through the various sections show that real life constraints have a significant impact on the algorithm design and the system response. Although in this small report a simplified analysis of a single input single output system was developed, appears straightforward that more powerful tools must be used to assure stability and good performances; especially for the supersonic jet system considered.

References

[1] R. B. J. H. Keviczky, L. and L. Cs. Bányász, *Control engineering.* Berlin: Springer, 2018.

[2] L. Horowitz IM, *Synthesis of feedback systems.* Academic Press, New York, 1963.

[3] L. Åström KJ, Wittenmark B, *Computer controlled systems. Theory and design.* Prentice Hall, Englewood Cliffs, 1984.

[4] L. Åström KJ, Murray RM, *Feedback systems: an introduction for scientists and engineers.* Princeton University Press, Princeton, 2008.